MOLECULAR AND CELLULAR BIOLOGY, Nov. 2004, p. 9630–9645 Vol. 24, No. 21
0270-7306/04/$08.00+0 DOI: 10.1128/MCB.24.21.9630–9645.2004

Human SWI/SNF-Associated PRMT5 Methylates Histone H3 Arginine 8 and Negatively Regulates Expression of *ST7* and *NM23* Tumor Suppressor Genes†

Sharmistha Pal,[1] Sheethal N. Vishwanath,[1] Hediye Erdjument-Bromage,[2] Paul Tempst,[2] and Saïd Sif[1]*

Department of Molecular and Cellular Biochemistry, College of Medicine and Public Health, The Ohio State University, Columbus, Ohio,[1] and Molecular Biology Program, Memorial Sloan-Kettering Cancer Center, New York, New York[2]

Received 29 June 2004/Returned for modification 15 July 2004/Accepted 28 July 2004

Protein arginine methyltransferases (PRMTs) have been implicated in transcriptional activation and repression, but their role in controlling cell growth and proliferation remains obscure. We have recently shown that PRMT5 can interact with flag-tagged BRG1- and hBRM-based hSWI/SNF chromatin remodelers and that both complexes can specifically methylate histones H3 and H4. Here we report that PRMT5 can be found in association with endogenous hSWI/SNF complexes, which can methylate H3 and H4 N-terminal tails, and show that H3 arginine 8 and H4 arginine 3 are preferred sites of methylation by recombinant and hSWI/SNF-associated PRMT5. To elucidate the role played by PRMT5 in gene regulation, we have established a PRMT5 antisense cell line and determined by microarray analysis that more genes are derepressed when PRMT5 levels are reduced. Among the affected genes, we show that *suppressor of tumorigenicity 7* (*ST7*) and *nonmetastatic 23* (*NM23*) are direct targets of PRMT5-containing BRG1 and hBRM complexes. Furthermore, we demonstrate that expression of *ST7* and *NM23* is reduced in a cell line that overexpresses PRMT5 and that this decrease in expression correlates with H3R8 methylation, H3K9 deacetylation, and increased transformation of NIH 3T3 cells. These findings suggest that the BRG1- and hBRM-associated PRMT5 regulates cell growth and proliferation by controlling expression of genes involved in tumor suppression.

During cell growth and proliferation several genes become either repressed or activated. These variations in expression often correlate with changes in chromatin structure, which can be induced by a variety of enzymes that can disrupt nucleosomes in an ATP-dependent manner and/or covalently modify nucleosomal histones (17, 29, 41, 58). Biochemical characterization of different members of the SWI2/SNF2 family of chromatin remodeling complexes revealed that there are complexes that can catalyze both ATP-dependent nucleosome disruption and histone deacetylation (48, 49, 55, 59). Unlike the nucleosome remodeling and deacetylase complex, human SWI/SNF (hSWI/SNF) complexes can be purified either alone or in combination with mSin3A/histone deacetylase, indicating that there are different pools of BRG1- and hBRM-based hSWI/SNF complexes (19, 27, 42). Recent work has also shown that flag-tagged BRG1 and hBRM complexes include the type II protein arginine methyltransferase 5 (PRMT5) and that these complexes are involved in transcriptional repression of the MYC/MAX/MAD target gene *CAD* (32). These studies and work by various groups suggest that ATP-dependent chromatin remodeling complexes can act in concert with various histone-modifying enzymes to modulate chromatin structure (10, 29). Although PRMT5 has been implicated in transcriptional repression of *CYCLIN E* and *CAD*, it is not clear whether it is involved in regulating a broader spectrum of genes and whether it has any effects on cell growth and proliferation.

Histone methylation has been identified as an important modification for both transcriptional activation and transcriptional repression. Thus far, it appears that there are two types of histone methyltransferases which include either a SET (Suvar3-9, Enhancer of Zeste, Trithorax) domain found primarily in proteins possessing lysine-specific methylase activity or an arginine-specific catalytic domain characteristic of PRMTs (18, 45, 58). Differential methylation of conserved lysine residues in histones H3 and H4 can lead to distinct transcriptional outcomes. For example, methylation of H3 lysine 4 (H3K4) by either SET7 or SET9 can activate transcription (30, 50), while methylation of H3K9 by either SUV39H1 or G9a can induce binding of heterochromatin protein 1 and promote transcriptional silencing by triggering the formation of heterochromatin (1, 22, 28, 31). Similarly, methylation of H3 arginine residues by PRMT4 has been shown to be involved in transcriptional activation, whereas methylation by PRMT5, which can target both H3 and H4, has been implicated in *CAD* and *CYCLIN E* transcriptional repression (4, 7, 32, 39). Currently, the histone residues modified by PRMT5 are still not known.

PRMTs can be divided into type I PRMTs, which catalyze monomethylation and asymmetric dimethylation of arginine residues, and type II PRMTs, which catalyze the formation of monomethylated and symmetrically dimethylated arginines (57). Among the six PRMT family members, only PRMT5 behaves as a type II PRMT that can target histones (3, 32, 34). Besides methylating and modulating the activity of proteins involved in nuclear export and signal transduction, PRMT1 and PRMT4 have also been shown to methylate histones H3

* Corresponding author. Mailing address: Department of Molecular and Cellular Biochemistry, Ohio State University College of Medicine, Columbus, OH 43210. Phone: (614) 247-7445. Fax: (614) 292-4118. E-mail: Sif.1@osu.edu.

† Supplemental material for this article may be found at http://mcb.asm.org/.

and H4 and activate transcription (4, 51). Although no PRMT2 substrates have been identified yet, it appears that PRMT2 can potentiate estrogen receptor transcriptional activity and that coactivation relies on the catalytic activity of PRMT2 (35). Both PRMT3 and PRMT6 can methylate cellular proteins, but their function in vivo remains unknown (8, 47).

PRMT5 was first identified in *Schizosaccharomyces pombe* as a protein that interacts and positively regulates Shk1 kinase, a member of the $p21^{Cdc42/Rac}$-activated kinases (PAKs), which play critical roles in RAS signaling (13). Deletion of *ras1* in fission yeast results in altered cell shape, and overexpression of PRMT5 partially restores wild-type morphology, indicating that PRMT5 is involved in RAS-induced cytoskeletal and morphological control pathways. Moreover, *prmt5*-null mutants grow slower and are less elongated than wild-type cells, and reexpression of either *S. pombe* or human PRMT5 rescues cell morphology, suggesting that PRMT5 is functionally conserved (12). Yeast two-hybrid screens have shown that PRMT5 can interact with a wide variety of proteins including Janus kinase 2 (Jak2), Orb6p kinase, and somatostatin receptors 1 and 4, implying that type II PRMTs might be targeted by or regulate components of different signaling modules (34, 40, 53). PRMT5 has also been shown to be part of a complex that can bind and methylate SmD1 and SmD3, which are involved in the biogenesis of spliceosomal U-rich snRNPs (9, 26). More recently, PRMT1 and PRMT5 were shown to interact and colocalize with the transcription elongation factor SPT5 on the IkBα and interleukin-8 promoters (20). Both arginine methyltransferases modify SPT5 and reduce its association with RNA polymerase II, suggesting that PRMT1 and PRMT5 might be involved in regulating transcriptional elongation. Further evidence in support of a role for PRMT5 in transcriptional repression comes from recent findings which show that PRMT5 is associated with the promoter region of genes that are either silent, such as interleukin-8, or have low basal activity, including IkBα, *CYCLIN E*, and *CAD* (7, 20, 32).

Our understanding of the mechanisms by which PRMT5 affects gene expression and cell growth and proliferation is very limited. We have previously reported the association of PRMT5 with flag-tagged BRG1 and hBRM complexes and shown that hSWI/SNF-associated PRMT5 can methylate hypoacetylated H3 and H4 more efficiently than the hyperacetylated forms. In this study, we provide further evidence to show that PRMT5 copurifies with endogenous BRG1 and hBRM complexes and demonstrate that immunopurified recombinant and hSWI/SNF-associated PRMT5 target the same H3 and H4 arginine residues. We also show that PRMT5 has the ability to stimulate cell growth and anchorage-independent growth by methylating H3R8 and reducing expression of genes involved in tumor suppression. These results indicate that the BRG1- and hBRM-associated PRMT5 is an important regulator of cell growth and proliferation.

MATERIALS AND METHODS

Plasmid constructions. Retroviral expression vectors for sense and antisense (AS) PRMT5 were generated using pBS(KS+)/flag-tagged PRMT5, which was previously described (32). Plasmid pBabe/Fl-PRMT5 was constructed by inserting a 2-kbp BamHI-EcoRI fragment, which was excised out of pBS(KS+)/Fl-PRMT5, into BamHI-EcoRI-linearized pBabe-puromycin. To generate the retroviral vector for knocking down PRMT5 expression, pBabe/AS-PRMT5, a PCR-amplified 1.1-kbp PRMT5 DNA fragment (+39 to +1140), was inserted in reverse orientation into pBabe-puromycin digested with BamHI and SalI. The 5′ primer (5′-ACGCGTCGACGTGATTGGCTACTAGTATCAAGGAATC-3′) was modified to include a SalI restriction site (underlined), while the 3′ primer (5′-CGCGGATCCCATATGTCTGAGATTCCAGATTGTC-3′) included a BamHI restriction site (underlined). For coupled in vitro transcription and translation of PRMT5, pBS(KS+)/Fl-PRMT5 was linearized with SacII to delete the flag-tag epitope. A retroviral vector for expression of catalytically inactive flag-tagged hBRM was constructed by excising a 5-kbp EcoRI DNA fragment from pBS(KS+)/CehBRM-NTP (6) and inserting it into EcoRI-linearized pBabe-puromycin.

Purification of endogenous and flag-tagged hSWI/SNF complexes, recombinant flag-tagged wild-type and mutant PRMT5, and mass spectrometry. To purify endogenous BRG1 and hBRM complexes, 300 mg of HeLa nuclear extract was loaded onto a 30-ml BioRex 70 column preequilibrated with BC100 (20 mM HEPES [pH 7.9], 100 mM KCl, 5 mM $MgCl_2$, 20% glycerol, 1 mM EDTA, 0.25 mM dithiothreitol, 0.5 mM phenylmethylsulfonyl fluoride). Next, bound proteins were eluted with BC100 buffer supplemented with increasing amounts of KCl, and the collected fractions were analyzed by Western blotting for the presence of PRMT5, BRG1, and hBRM. Peak fractions (0.5 M and 0.8 M KCl) containing PRMT5 and hSWI/SNF complexes were pooled and dialyzed against BC100 before they were loaded on two separate DE 52 columns. Both columns were eluted as described for the BioRex 70 column, and the collected fractions were analyzed by Western blotting for the presence of PRMT5-containing hSWI/SNF complexes. The 0.3 M KCl fractions from both DE 52 columns, which contained the majority of endogenous hSWI/SNF complexes, were used in immunoprecipitation assays. Approximately 100 μg of each pooled peak fraction was incubated with 10 μl of either preimmune or immune anti-PRMT5 antibodies at 4°C for 4 h. Next, protein A agarose beads preblocked in 0.5 mg of bovine serum albumin (BSA)/ml overnight at 4°C were added to each reaction mixture. Samples were incubated at 4°C for 8 to 10 h, and beads were collected and washed three times with 1 ml of washing buffer (40 mM Tris-HCl [pH 8.0], 250 mM NaCl, 0.5% NP-40). Bound proteins were separated on a sodium dodecyl sulfate (SDS)–8% polyacrylamide gel and analyzed by Western blotting. Flag-tagged hSWI/SNF complexes and Sf9-expressed flag-tagged wild-type and mutant PRMT5 were purified as described previously (32, 42, 43). The gel-purified 70-kDa band in the HeLa and INI1 fractions was identified by mass spectrometry as described previously (32).

In vitro translation and immunoprecipitation assays. PRMT5 was synthesized in vitro by incubating 2 μg of linearized plasmid DNA with 25 μl of TNT-coupled rabbit reticulocyte lysate in the presence of [^{35}S]methionine and cysteine (NEN) according to the manufacturer's instructions (Promega). In vitro-translated PRMT5 was immunoprecipitated by incubating approximately 60×10^3 to 70×10^3 cpm with antibodies in a 250-μl reaction mixture containing immunoprecipitation buffer (20 mM Tris-HCl [pH 7.4], 100 mM NaCl, 5 mM $MgCl_2$, 1 mM EDTA, 0.05% NP-40, 1% aprotinin). After a 1-h incubation on ice, 75 μl of a 50% slurry of protein A agarose beads was added, and the reaction mixture was incubated overnight at 4°C. Samples were washed as described for immunopurified hSWI/SNF complexes, and bound proteins were analyzed by SDS-polyacrylamide gel electrophoresis and autoradiography.

Histone and peptide methylation assays. Methylation assays were performed using either HeLa core histones (2.5 μg), acetylated or nonacetylated histone N-terminal peptides (4 μg), and Sf9-expressed recombinant flag-tagged PRMT5 (250 ng) or hSWI/SNF-associated PRMT5 (400 ng) in a 25-μl reaction mixture containing 15 mM HEPES (pH 7.9), 100 mM KCl, 5 mM $MgCl_2$, 20% glycerol, 1 mM EDTA, 0.25 mM dithiothreitol, 0.5 mM phenylmethylsulfonyl fluoride, and 2.75 μCi of *S*-[^{3}H]adenosylmethionine (SAM) (Amersham Pharmacia Biotech., Inc.). After a 1.5-h incubation at 30°C, HeLa core histones were visualized as described previously (32). When acetylated peptides were used, reaction mixtures were supplemented with 40 mM sodium butyrate. Reaction mixtures containing histone N-terminal peptides were spotted on Whatman P-81 filter paper and washed five times with 10 ml of 0.1 M sodium carbonate buffer (pH 9.0) to remove unincorporated [^{3}H]SAM. Methylated peptides were detected by scintillation counting.

Cell culture, proliferation, and transformation assays. HeLa S3, NIH 3T3, and flag-tagged dominant-negative BRG1 and hBRM cell lines were cultured in Dulbecco's modified Eagle's medium containing 10% fetal bovine serum. HeLa S3 and flag-tagged INI1-11 cell lines were grown at the National Cell Culture Center (Biovest International, Inc.). HeLa S3 cell lines that express dominant-negative flag-tagged BRG1 were described previously (42). HeLa S3 cell lines that express mutant flag-tagged hBRM were generated as described previously (43). To generate cell lines that express Fl-PRMT5, AS-PRMT5, or MYC and RAS, 5×10^5 NIH 3T3 cells were transfected for 5 h with 2 μg of pBabe/Fl-PRMT5, pBabe/AS-PRMT5, or pBabe-hygromycin/MYC and pBabe-hygromy-

cin/RAS by using Lipofectamine (Invitrogen, Inc.). Two days after transfection, drug-resistant cells expressing either Fl-PRMT5, AS-PRMT5, or MYC/RAS were selected for 2 weeks in the presence of either 3 μg of puromycin/ml or 480 U of hygromycin/ml. For NIH 3T3 cells expressing AS-PRMT5, several individual colonies were isolated, expanded into cell lines, and analyzed by reverse transcriptase PCR (RT-PCR) as well as Western blotting to assess endogenous PRMT5 levels. After several clones were screened, NIH 3T3/AS-PRMT5 clone 15 was used in subsequent experiments because expression of endogenous PRMT5 was reduced by more than 90% as quantitated by RT-PCR.

To measure the proliferation rate of different cell lines, 2×10^5 cells were seeded into 6-cm-diameter plates and allowed to grow for 6 days. Proliferation of each cell line was repeated three times with duplicate plates, and cells were counted every 2 days. To measure bromodeoxyuridine (BrdU) incorporation, 10^6 cells were treated with 10 μM BrdU for either 4.5 or 9 h according to the instructions of the manufacturer (Becton Dickinson). Next, cells were incubated with 1 μl of fluorescein isothiocyanate-conjugated anti-BrdU antibody that was diluted 1:50 in supplied 1× BD Perm/Wash buffer. Samples were then washed twice with 1 ml of 1× BD Perm/Wash buffer and resuspended in 1 ml of staining buffer containing 20 μl of 7-amino-actinomycin D before cells were analyzed by fluorescence-activated cell sorting (FACS) analysis. To determine if NIH 3T3 cells expressing AS-PRMT5 were undergoing apoptosis, 2×10^5 cells were plated and allowed to grow for 4 days before the DNA content was examined by FACS analysis with a FACScalibur flow cytometer (Becton Dickinson).

To assess the anchorage-dependent growth potential of NIH 3T3/Fl-PRMT5 and NIH 3T3/AS-PRMT5, 4×10^3 cells were plated in 10-cm-diameter plates. After 7 days, colonies were visualized by fixing the cells in 10% buffered formalin solution and staining them with 0.1% crystal violet. For analysis of anchorage-independent growth, 2×10^2 cells were seeded into 6-cm-diameter plates in Dulbecco's modified Eagle's medium containing 0.3% agar as described previously (11). Each cell line was tested for its ability to grow in soft agar by using triplicate plates. Colonies were counted, and the average from three different experiments is shown.

RT-PCR and microarray analyses. RNA was prepared from NIH 3T3, NIH 3T3/AS-PRMT5, NIH 3T3/Fl-PRMT5, HeLa S3, flag-tagged dominant-negative BRG1, and flag-tagged dominant-negative hBRM cell lines by using Trizol reagent (Invitrogen, Inc.) according to the manufacturer's instructions. Approximately 10 to 20 μg of total RNA was used in a 20-μl reaction mixture containing 20 pmol of specific 3′ primer, 3.5 mM $MgCl_2$, 1 mM deoxynucleoside triphosphates, 1× Taq Pol buffer (Invitrogen, Inc.), 15 U of avian myeloblastosis virus RT (Promega, Inc.), and 2.5 U of RNasin. Either 0.2 μl or 2.0 μl of the RT reaction mixture was PCR amplified using specific primers in a 50-μl reaction mixture containing 2.5 U of *Taq* polymerase (Invitrogen, Inc.) and 2 μCi of [α-^{32}P]dCTP. Amplified fragments were separated from nonspecific products by electrophoresis on a 5% polyacrylamide gel and quantitated with a Molecular Dynamics PhosphorImager. Specific primer pairs were used to amplify the following genes: *NM23* (+103 to +313), *ST7* (+448 to +717), *RRM1* (+181 to +591), *CYCLIN B2* (+172 to +489), *CYCLIN E2* (+69 to +409), NF-κB (+393 to +762), *GAS2* (+275 to +595), *CDC20* (+161 to +540), *CDK4* (+151 to +542), *MYT1l* (+796 to +1112), *ALL1* (+186 to +432), *SERPIN E1* (+368 to +798), *PRMT5* (+1093 to +1306), glyceraldehyde-3-phosphate dehydrogenase (*GAPDH*) (+178 to +578), and β-*ACTIN* (+140 to +585).

Microarray analysis was performed using 10 μg of total RNA isolated from either puromycin-resistant NIH 3T3 or NIH 3T3/AS-PRMT5 cells. Affymetrix MG-U74Av2 high-density expression array chips, which include 6,000 cDNA clones and 8,000 expressed sequence tags, were used to identify genes whose expression was altered when PRMT5 levels were reduced. The analysis was performed by the Ohio State University Comprehensive Cancer Center microarray facility (http://www.dnaarrays.org). Gene expression levels were estimated from GeneChip PM probe intensities by means of an enhanced two-array version of the Li-Wong PM-only algorithm (5). The enhanced algorithm (i) scales all PM and MM probe intensities so as to minimize between-array differences in the scaled MM probe intensity distributions, (ii) applies between-array variance analysis to the scaled PM probe intensities in order to estimate PM-specific sensitivities, (iii) estimates gene expression levels by regressing scaled PM probe intensities on estimated PM probe sensitivities within each probe set, and (iv) tests a probe-level general linear model within each probe set in order to estimate the *P* values for between-array differential gene expression. The estimated *P* values can be several orders of magnitude lower than 0.05, as required by the Bonferroni correction, which applies when simultaneously testing thousands of genes for significant differential expression (16).

Antibodies and Western blot analysis. Proteins were separated on an SDS–8 to 10% polyacrylamide gel, transferred onto nitrocellulose, and detected using anti-hSWI/SNF subunits, anti-PRMT5, and anti-flag M2 rabbit polyclonal antibodies, which have been described previously (32, 42, 43). To test anti-H3(Me_2)R8 antibodies, which were generated by Covance, Inc., methylated and unmethylated H3 peptides were spotted on nitrocellulose before Western blots were developed using ECL reagent (Pharmacia Amersham Biotech. Inc.). Anti-MAD and anti-H3AcK9 were purchased from Santa Cruz Biotechnology and Upstate Biotechnology, respectively.

Chromatin immunoprecipitation (ChIP) assay. Cross-linked chromatin was prepared as described previously (32). Briefly, 90 to 95% confluent 10-cm-diameter plates were treated with 1% formaldehyde for 10 min at room temperature and harvested in 1 ml of lysis buffer (50 mM Tris-HCl [pH 8.1], 100 mM NaCl, 5 mM EDTA, 0.5% SDS, protease inhibitors) after glycine was added to a final concentration of 0.1 M. Chromatin was collected by centrifugation and resuspended in 250 μl of immunoprecipitation buffer (100 mM Tris-HCl [pH 8.6], 5 mM EDTA, 0.3% SDS, 1.7% Triton X-100, protease inhibitors) before it was sonicated. Solubilized bulk chromatin, which contained DNA fragments that varied in size from 0.25 to 1.5 kbp, was immunoprecipitated using specific antibodies in the presence of 40 μl of preblocked protein A beads (0.5 mg of BSA/ml, 0.2 mg of salmon sperm DNA/ml) at 4°C for 14 h. Bound nucleoprotein complexes were washed successively with 300 μl of mixed micelle buffer (20 mM Tris-HCl [pH 8.1], 100 mM NaCl, 5 mM EDTA, 5% [wt/vol] sucrose, 0.2% Triton X-100, 0.2% SDS), buffer 250 (50 mM HEPES [pH 7.5], 250 mM NaCl, 1 mM EDTA, 0.1% deoxycholine, 0.2% Triton X-100), LiCl detergent buffer (10 mM Tris-HCl [pH 8.0], 250 mM LiCl, 1 mM EDTA, 0.5% deoxycholine, 0.25% NP-40), and Tris-EDTA (pH 7.6). After phenol and chloroform extraction, DNA was resuspended in 30 μl of Tris-EDTA (pH 7.6). Specific primers were used to amplify promoter sequences in a 50-μl reaction mixture containing 2 μCi of [α-P^{32}]dCTP.

RESULTS

PRMT5 can interact with endogenous BRG1- and hBRM-based hSWI/SNF complexes. We have previously shown using flag-tagged BRG1 and hBRM cell lines that PRMT5 can be found in association with affinity-purified hSWI/SNF complexes (32). To rule out the possibility that PRMT5 interacted with hSWI/SNF complexes only when BRG1 and hBRM were overexpressed, we analyzed its association with endogenous hSWI/SNF complexes (Fig. 1). HeLa nuclear extracts were fractionated on a BioRex 70 column, and the eluted proteins were analyzed by Western blotting with anti-PRMT5, anti-BRG1, and anti-hBRM antibodies. Previous work has shown that BRG1- and hBRM-based hSWI/SNF complexes copurify on phosphocellulose 11 (21). Consistent with these results, we found that BRG1 and hBRM coelute at 0.5 M and 0.8 M KCl. In addition, PRMT5 cofractionates with both chromatin remodeling ATPases. When both hSWI/SNF-enriched fractions were further purified on a DE 52 column, PRMT5 coeluted with BRG1 and hBRM at 0.3 M KCl, suggesting that it is in complex with endogenous BRG1 and hBRM ATPases. To demonstrate that PRMT5 is tightly associated with hSWI/SNF complexes, we immunoprecipitated partially purified BRG1 and hBRM complexes with either preimmune or immune anti-PRMT5 antibodies and tested for the presence of BRG1 and hBRM by Western blotting. Both BRG1 and hBRM coimmunoprecipitated with PRMT5 in the presence of 0.3 M KCl, indicating that PRMT5 is tightly associated with endogenous BRG1- and hBRM-based hSWI/SNF complexes. Similar results were observed when flag-tagged INI1 nuclear extracts were fractionated on BioRex 70, DE 52, Mono S, and anti-flag M2 columns, further supporting the specific and tight association of PRMT5 with BRG1 and hBRM complexes (data not shown).

Although purification by conventional chromatography can allow us to monitor association of PRMT5 with hSWI/SNF complexes, the amount of active fractions purified by this

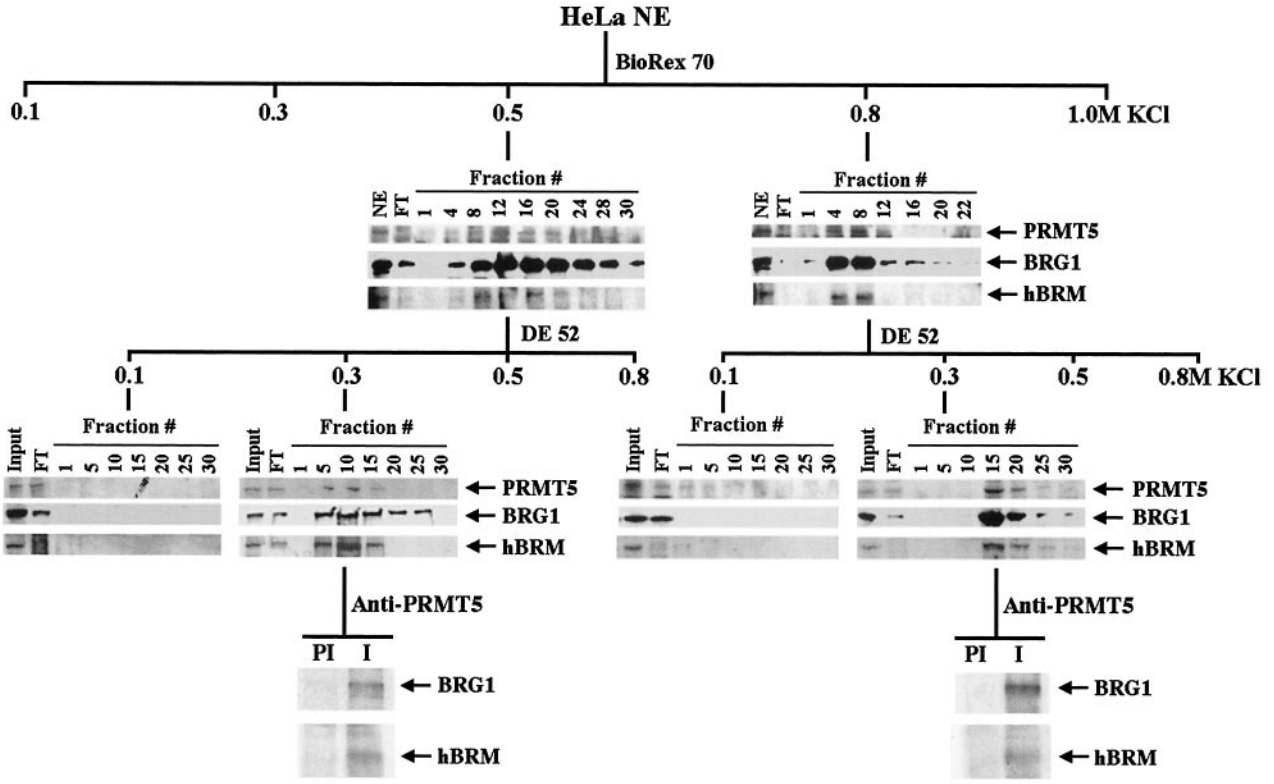

FIG. 1. PRMT5 coelutes with endogenous BRG1 and hBRM complexes. HeLa nuclear extracts (300 mg) were loaded on a 25-ml BioRex 70 column. After the flowthrough (FT) was collected, the column was washed with increasing salt concentrations as indicated. Fractions were collected and analyzed by Western blotting with either anti-PRMT5, anti-BRG1, or anti-hBRM antibodies. Peak fractions from the BioRex 70 column (fractions 4 to 28 for the 0.5 M KCl elution and fractions 4 to 12 for the 0.8 M KCl elution) were pooled and dialyzed against BC100 buffer. Dialyzed proteins were loaded on two DE 52 columns and eluted as described for the BioRex 70 column. Peak fractions (0.3 M KCl) were pooled and immunoprecipitated using either preimmune (PI) or immune (I) anti-PRMT5 antibodies. After extensive washing, proteins were analyzed by Western blotting with the indicated antibodies.

method is very limiting. Therefore, we used the flag-tagged INI1-11 cell line to purify PRMT5-containing BRG1 and hBRM complexes (43). Fl-INI1 or HeLa nuclear extracts were incubated with anti-flag M2 affinity gel, and after extensive washing the retained proteins were eluted with flag peptide. The collected fractions were then analyzed by silver staining and Western blotting (Fig. 2A and B). In addition to the previously identified hSWI/SNF subunits, PRMT5 was enriched in fractions containing BRG1 and hBRM but not in control fractions purified using HeLa nuclear extract (Fig. 2B). To rule out the possibility that PRMT5 interacted nonspecifically with flag antibody, we conducted immunoprecipitation experiments in the absence of hSWI/SNF subunits. In vitro-translated and ^{35}S-labeled PRMT5 was incubated with either agarose beads, anti-flag M2 beads, or preimmune or immune anti-PRMT5 antibodies. As expected, PRMT5 was immunoprecipitated only in the presence of anti-PRMT5 antibodies, indicating that PRMT5 does not cross-react with anti-flag antibody (Fig. 2C). We have also identified PRMT5 by mass spectrometry in the immunopurified Fl-hSWI/SNF complexes but not in the HeLa fraction (data not shown). These results are in complete agreement with our previous results, which show that PRMT5 can interact with specific hSWI/SNF subunits (32), and confirm the association of PRMT5 with endogenous hSWI/SNF complexes.

hSWI/SNF-associated PRMT5 preferentially methylates H3 arginine 8 and H4 arginine 3 and is inhibited by either H3K9 or K14 acetylation. PRMT5 is a type II arginine methyltransferase that can target proteins involved in signal transduction, transcriptional elongation, and splicing (9, 20, 26, 34). More recently, PRMT5 has also been shown to methylate histones; however, the identity of its target sites remains unknown. Using immunopurified flag-tagged hSWI/SNF (Fl-hSWI/SNF) complexes, we examined whether PRMT5 could methylate H1-depleted HeLa core histones in the presence of [^{3}H]SAM (Fig. 2C). BRG1- and hBRM-associated PRMT5 was able to methylate histones H3 and H4 but not H2A and H2B. Similarly, when Sf9-expressed and affinity-purified flag-tagged wild-type PRMT5 (Fl-PRMT5) was incubated with the four core histones, both H3 and H4 were methylated. In contrast, catalytically inactive Fl-PRMT5(G367A/R368A) was unable to methylate HeLa core histones. It is important to note based on Western blot analysis and silver staining that seven- to nine-fold-more recombinant Fl-PRMT5 was required to detect H3 and H4 methylation (Fig. 2D and data not shown), suggesting that association with BRG1 and hBRM complexes enhances PRMT5 methylase activity.

Most regulatory histone posttranslational modifications occur in the N-terminal tails of histones H3 and H4 (17, 45, 58). To test whether hSWI/SNF-associated PRMT5 could methyl-

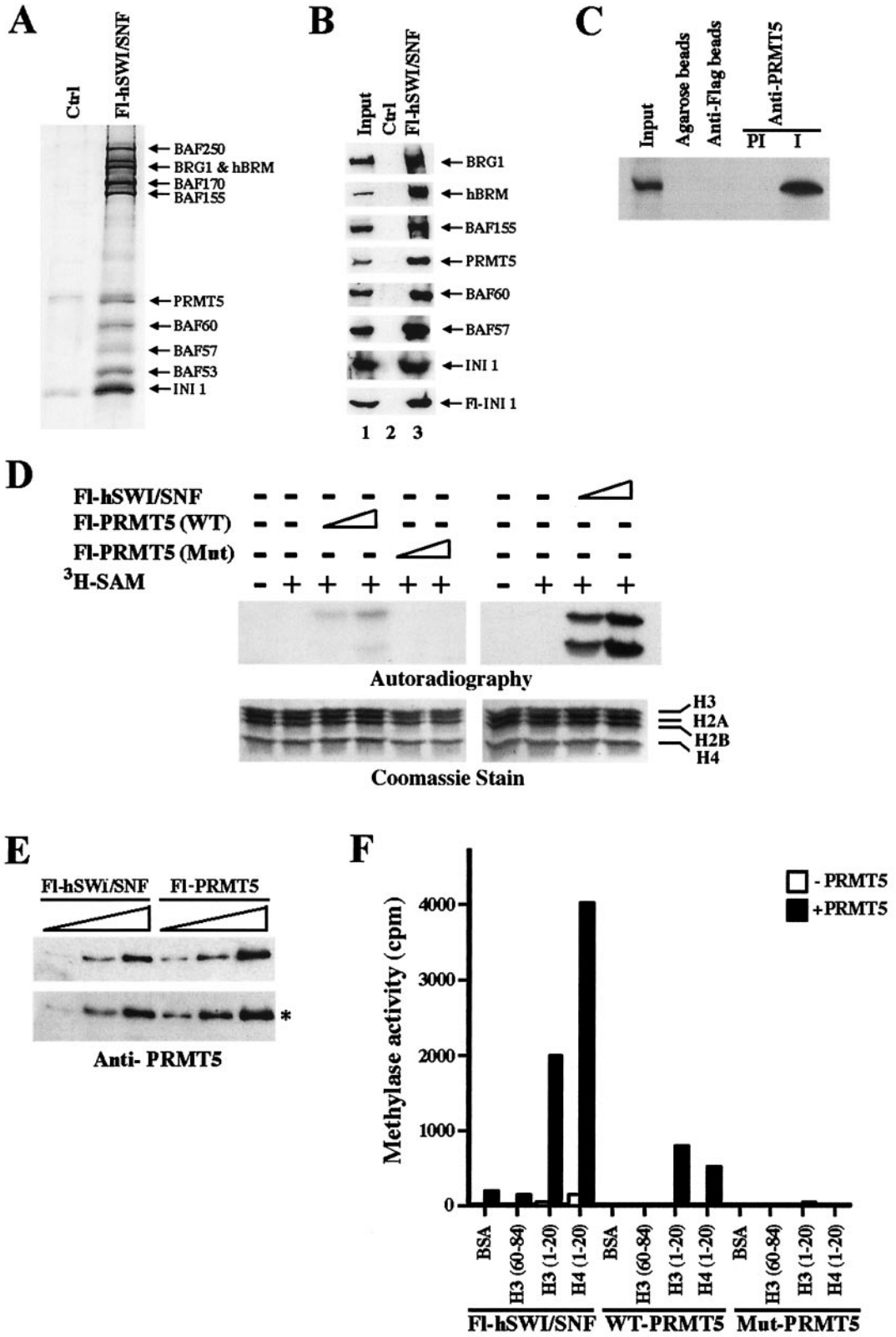

FIG. 2. PRMT5 coelutes with flag-tagged INI1 complexes. Either HeLa S3 or Fl-INI1 nuclear extract (180 mg) was incubated with anti-flag M2 affinity gel, and hSWI/SNF complexes were eluted with a 20-fold molar excess of flag peptide. Eluted complexes were analyzed by silver staining (A) or by Western blotting (B) with specific antibodies. Western blot assays were performed using 20 μg of Fl-INI1 nuclear extract (Input, lane 1), 15 μl of eluted fraction with HeLa nuclear extract (Ctrl, lane 2), and 15 μl of eluted flag-tagged hSWI/SNF (Fl-hSWI/SNF) complexes (lane 3). (C) PRMT5 does not cross-react with anti-flag antibodies. In vitro-translated and ^{35}S-labeled PRMT5 was incubated with either agarose beads or anti-flag M2 antibody cross-linked to agarose beads. As a control, preimmune (PI) and immune (I) anti-PRMT5 antibodies were also included.

ate histone N-terminal tails, we used highly purified peptides (>95% purity) that encompass the first 20 amino acids (aa) of histones H3 and H4 in methylation assays. Both recombinant and hSWI/SNF-associated PRMT5 were able to specifically methylate N-terminal H3 and H4 peptides but not BSA or a control peptide, which contains four arginine residues within the globular domain of histone H3 (aa 60 to 84) (Fig. 2E). Catalytically inactive Fl-PRMT5(G367A/R368A) was unable to methylate H3 and H4 N-terminal tails. These results show that H3 and H4 methylation is catalyzed by PRMT5 and is not due to the presence of a contaminating histone methyltransferase.

Since PRMT5 is an arginine-specific methylase, we sought to identify its target sites in the H3 and H4 N-terminal tails. We used H3 and H4 peptides with specific arginine-to-alanine mutations as substrates in methylation assays (Fig. 3). When hSWI/SNF-associated PRMT5 was incubated with equal amounts of unlabeled wild-type and mutant peptides, only H3R8A and H3R2A/R8A/R17A were not methylated (Fig. 3A). Both single-point mutant peptides, H3R2A and H3R17A, were efficiently methylated by hSWI/SNF-associated PRMT5, suggesting that neither H3R2 nor H3R17 is critical for PRMT5-mediated H3 methylation. To further confirm the specificity of hSWI/SNF-associated PRMT5 for H3R8, we tested recombinant Fl-PRMT5 for its ability to methylate wild-type and mutant H3 peptides (Fig. 3B). Fl-PRMT5 was able to methylate wild-type H3, H3R2A, and H3R17A but not H3R8A and H3R2A/R8A/R17A, indicating that H3 arginine 8 is the primary site of methylation by PRMT5. A similar approach was used to identify the H4 arginine residues methylated by PRMT5 (Fig. 3C and D). When either recombinant or hSWI/SNF-associated PRMT5 was incubated with H4 N-terminal peptides bearing an R3A substitution, there was a lack of methylation, suggesting that H4 arginine 3 is preferentially methylated by PRMT5. Taken together, these results show that recombinant and hSWI/SNF-associated PRMT5 targets specific arginine residues in the H3 and H4 N-terminal tails.

Previous work has shown that H3K9 methylation interferes with lysine acetylation, and we have recently shown that hyperacetylated HeLa core histones are not efficiently methylated by BRG1- and hBRM-associated PRMT5 (32, 36). To assess whether acetylation of conserved H3 lysine residues could affect PRMT5-mediated arginine methylation, we used acetylated H3 peptides as a substrate in methylation assays (Fig. 3E). Both acetylated H3K9 and H3K14 were not methylated by hSWI/SNF-associated PRMT5, indicating that H3 lysine acetylation inhibits arginine 8 methylation.

Identification of genes regulated by PRMT5. PRMT5 has been implicated in the control of yeast cell morphology by interacting with the Shk1 kinase, which is involved in Ras- and Cdc42-dependent signaling. Little, however, is known about its role in the control of cell cycle progression and proliferation in mammalian cells. Having determined that PRMT5 can methylate specific arginine residues in the H3 and H4 N-terminal tails, we wanted to identify its target genes and investigate its effect on their expression. We, therefore, established an antisense NIH 3T3 cell line where *PRMT5* transcript levels were reduced by more than 90% as measured by RT-PCR (Fig. 4A). When we measured *GAPDH* mRNA levels, there was no noticeable change, and similarly transcription of β-*ACTIN* was not affected in the antisense PRMT5 cell line (data not shown). To determine whether transcription of the antisense construct can decrease PRMT5 protein levels, we performed Western blot analysis. In agreement with the RT-PCR results, endogenous PRMT5 levels were reduced 2.6-fold in the antisense cell line, while MAD levels were unaffected (Fig. 4B). These results demonstrate that the antisense construct can specifically reduce *PRMT5* expression.

To identify genes regulated by PRMT5, we performed a comparative microarray analysis with RNA from puromycin-resistant NIH 3T3 and antisense PRMT5 cell lines. We found that 227 genes were up-regulated, while only 43 genes were down-regulated, suggesting that more genes are repressed by PRMT5 (see Tables S1 and S2 in the supplemental material). The list of differentially expressed sequences included genes involved in cell adhesion and signaling, cell cycle progression, metabolic pathways, protein degradation, and chromatin remodeling. Several genes involved in promoting cell cycle progression, as well as genes exhibiting antiproliferative properties, were derepressed in the antisense cell line, suggesting that PRMT5 negatively regulates their expression. Among the genes with tumor suppressor activity, *suppressor of tumorigenicity 7* (*ST7*), *nonmetastatic 23* (*NM23*), *growth arrest specific 1* and *2* (*GAS1* and *GAS2*, respectively), *lysyl oxidase-like* (*LOXl*), and *retinoblastoma like-1* (p107) were derepressed 2.5- to 5-fold. Similarly, cell cycle regulators such as *CDK4*, *CYCLIN B2*, *CYCLIN E2*, and *CDC20* were also induced two- to fourfold in the antisense cell line (see Table S1 in the supplemental material). To verify whether the transcript levels of genes identified by microarray analysis were truly affected by reduced expression of *PRMT5*, we performed RT-PCR analysis on a group of genes that were either up- or down-regulated (Fig. 4C and D). All tumor suppressor and cell cycle inducer genes were derepressed to the same extent as determined by microarray analysis. Similarly, activation-deficient genes such as *myelin transcription factor 1-like* (*MYT1l*), *ALL1-fused gene from chromosome 1q* (*ALL1*), and *serine proteinase inhibitor E1* (*SERPIN E1*) were also affected three- to fourfold, which is consistent

The immunoprecipitated complexes were washed as described for panel A and visualized by autoradiography. (D) Recombinant and hSWI/SNF-associated PRMT5 can methylate histones H3 and H4. H1-depleted HeLa core histones were incubated with either Fl-hSWI/SNF complexes, affinity-purified wild-type (WT) Fl-PRMT5, or mutant (Mut) Fl-PRMT5/G367A-R368A in the presence of [^{3}H]SAM. Histones were visualized by Coomassie blue staining, and methylated products were detected by autoradiography. (E) Levels of PRMT5 in Fl-hSWI/SNF complexes were quantitated by Western blot analysis with increasing amounts of either immunopurified Fl-hSWI/SNF fractions (100, 200, and 400 ng) or Sf9-expressed and affinity-purified Fl-PRMT5 (6.25, 12.5, and 25 ng). The asterisk indicates a long exposure of the anti-PRMT5 Western blot. (F) Methylation of histone H3 and H4 N-terminal tails was carried out as described for panel D. Reaction mixtures were spotted onto Whatman P-81 filter paper, and methylated peptides were quantitated by liquid scintillation counting as described in Materials and Methods. As controls, methylation of BSA and H3 peptide (aa 60 to 84) is shown.

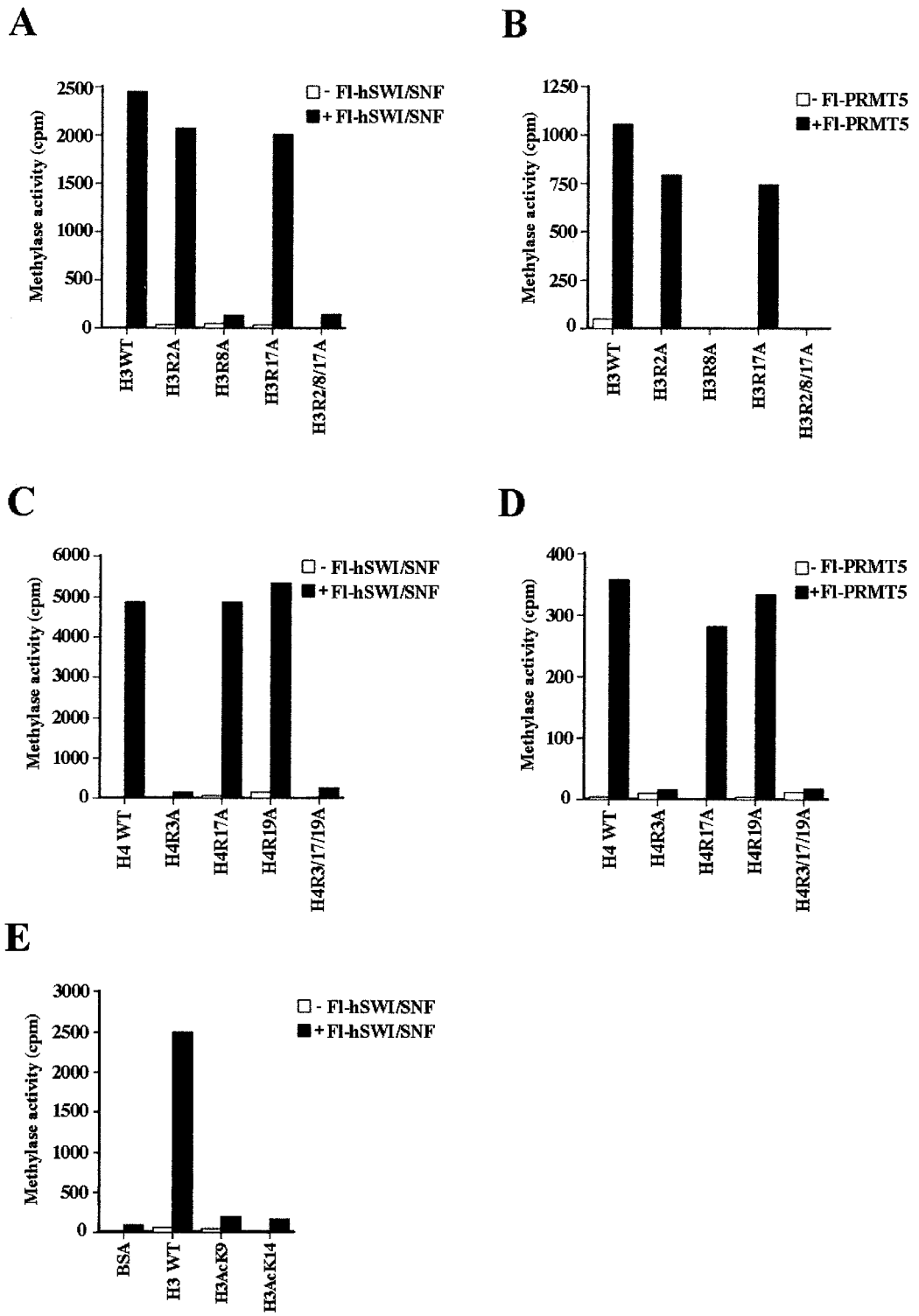

FIG. 3. Recombinant and hSWI/SNF-associated PRMT5 can specifically methylate H3R8 and H4R3. Wild-type and mutant H3 peptides containing an arginine-to-alanine mutation at a single position (2, 8, or 17) or at all three positions were incubated with either Fl-hSWI/SNF complexes (A) or flag-tagged wild-type PRMT5 (B) in the presence of [^{3}H]SAM. Similarly, wild-type and mutant H4 peptides with either a single point mutation (R3A, R17A, or R19A) or a triple point mutation (R3A/R17A/R19A) were incubated with either Fl-hSWI/SNF complexes (C) or Fl-PRMT5 (D), and samples were processed as described for Fig. 2E. (E) H3 peptides acetylated at K9 or K14 were incubated with Fl-hSWI/SNF as described above. As controls, BSA and wild-type H3 peptide are shown.

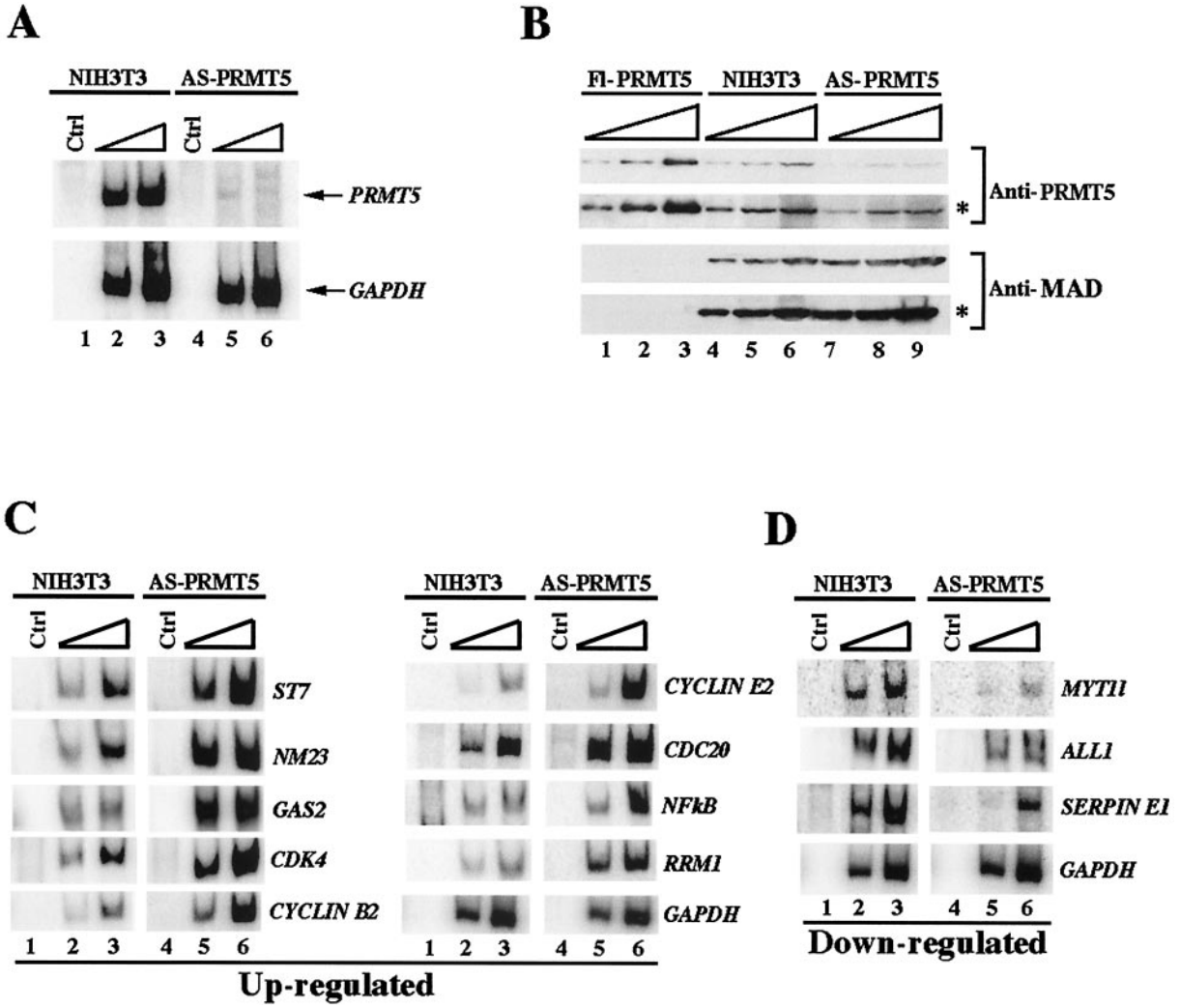

FIG. 4. Characterization of sense and antisense (AS) PRMT5 cell lines. (A) Expression of endogenous PRMT5 was assessed in NIH 3T3 and AS-PRMT5 cell lines. RT-PCR was performed using 20 μg of total RNA from either NIH 3T3 cells (lanes 1 to 3) or AS-PRMT5 cells (lanes 4 to 6) with primers specific for either *PRMT5* or *GAPDH*. PCRs were performed using 2 μl (lanes 1, 3, 4, and 6) or 0.2 μl (lanes 2 and 5) of the respective 20-μl RT reaction mixtures. Control (Ctrl) represents PCRs lacking the 5′ primer (lanes 1 and 4). Primers used to determine the PRMT5 transcript levels were placed downstream (+1093 to +1306) from the sequences used to knock down PRMT5 (+39 to +1165). (B) Increasing amounts (10, 20, and 40 μg) of whole-cell extracts from NIH 3T3 and AS-PRMT5 cells were analyzed by Western blotting with anti-PRMT5 and anti-MAD antibodies. For quantitation purposes, increasing amounts (6.25, 12.5, and 25 ng) of Sf9-expressed and affinity-purified Fl-PRMT5 were analyzed on the same blot. The asterisks indicate long exposures of anti-PRMT5 and anti-MAD Western blots. (C and D) RT-PCR was conducted as described for panel A with primers specific for the indicated up-regulated genes (C) and down-regulated genes (D). As a control, *GAPDH* levels were also analyzed.

with the transcription profiling results (see Table S2 in the supplemental material). Thus, PRMT5 regulates expression of genes whose expression has been shown to be altered in different human cancers.

PRMT5 stimulates cell proliferation and induces anchorage-independent growth. Since PRMT5 negatively regulates expression of cell cycle inducers as well as tumor suppressor genes, we examined its effect on cell growth and proliferation by establishing a cell line that overexpresses flag-tagged PRMT5 (Fl-PRMT5) and comparing its growth characteristics to those of the antisense PRMT5 (AS-PRMT5) cell line (Fig. 5A and B). In comparison to NIH 3T3, AS-PRMT5 cells grew two- to threefold slower, indicating that PRMT5 is required for normal cell growth and proliferation. In stark contrast, cells overexpressing Fl-PRMT5 grew three- to fourfold faster than NIH 3T3 cells, and their proliferation rate paralleled that of MYC/RAS-transformed NIH 3T3 cells. To understand why AS-PRMT5 and Fl-PRMT5 behaved differently and showed different growth characteristics, we measured their ability to incorporate BrdU and analyzed their DNA content by FACS analysis (Fig. 5C and D). AS-PRMT5 cells did not incorporate BrdU as efficiently as did NIH 3T3 and Fl-PRMT5 cells and showed no evidence of cell death. These results suggest that reduced proliferation of AS-PRMT5 cells is not due to induced cell death but rather to a slow transition from G_1 to S phase.

Because Fl-PRMT5 cells had a higher proliferation rate, a characteristic of transformed cells, we tested whether overexpression of PRMT5 could promote colony formation (Fig. 6A).

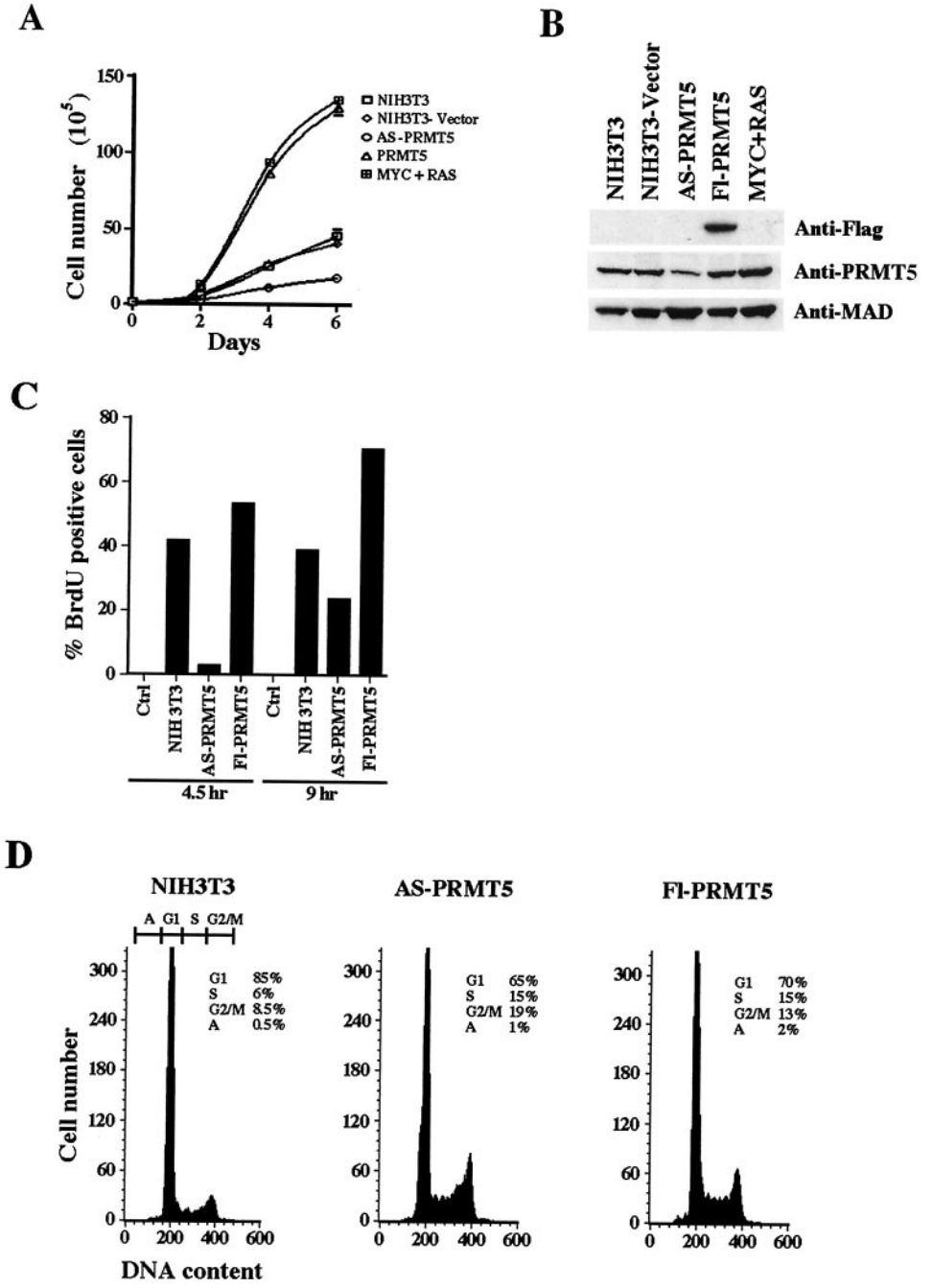

FIG. 5. PRMT5 induces cell growth and proliferation. (A) Proliferation of NIH 3T3, puromycin-resistant stable cell lines that express AS-PRMT5 or Fl-PRMT5, or hygromycin-resistant MYC/RAS-transformed NIH 3T3 cells was measured using 2×10^5 cells as described in Materials and Methods. The experiment was repeated three times, and the data points represent the average count from six plates. Standard deviations are included but are too small for the error bars to appear on the graph. (B) Approximately 40 μg of whole-cell extract from the indicated cell lines was analyzed by Western blotting with anti-flag antibodies to detect expression of Fl-PRMT5 in the flag-tagged PRMT5 cell line. The same blot was stripped and probed with either anti-PRMT5 or anti-MAD antibodies. (C) BrdU incorporation in NIH 3T3, AS-PRMT5, and Fl-PRMT5 cells was determined after 4.5 or 9 h of incubation with BrdU as described in Materials and Methods. The percentage of BrdU-positive cells was determined by FACS analysis. (D) NIH 3T3, AS-PRMT5, and Fl-PRMT5 cells were grown for 4 days and stained with propidium iodide, and the DNA content of each cell line was analyzed by FACS analysis. The percentage of cells in each stage of the cell cycle including cells undergoing apoptosis (A) is shown.

When equal numbers of sense and antisense PRMT5 cells were cultured in an anchorage-dependent manner, only cells that overexpressed Fl-PRMT5 were able to form colonies at a rate comparable to that of MYC/RAS-transformed cells. Similarly, when sense and antisense PRMT5 cells were cultured in soft agar, both Fl-PRMT5 and MYC/RAS-transformed cells were able to form colonies. However, antisense PRMT5 and NIH 3T3 cells were unable to grow in an anchorage-indepen-

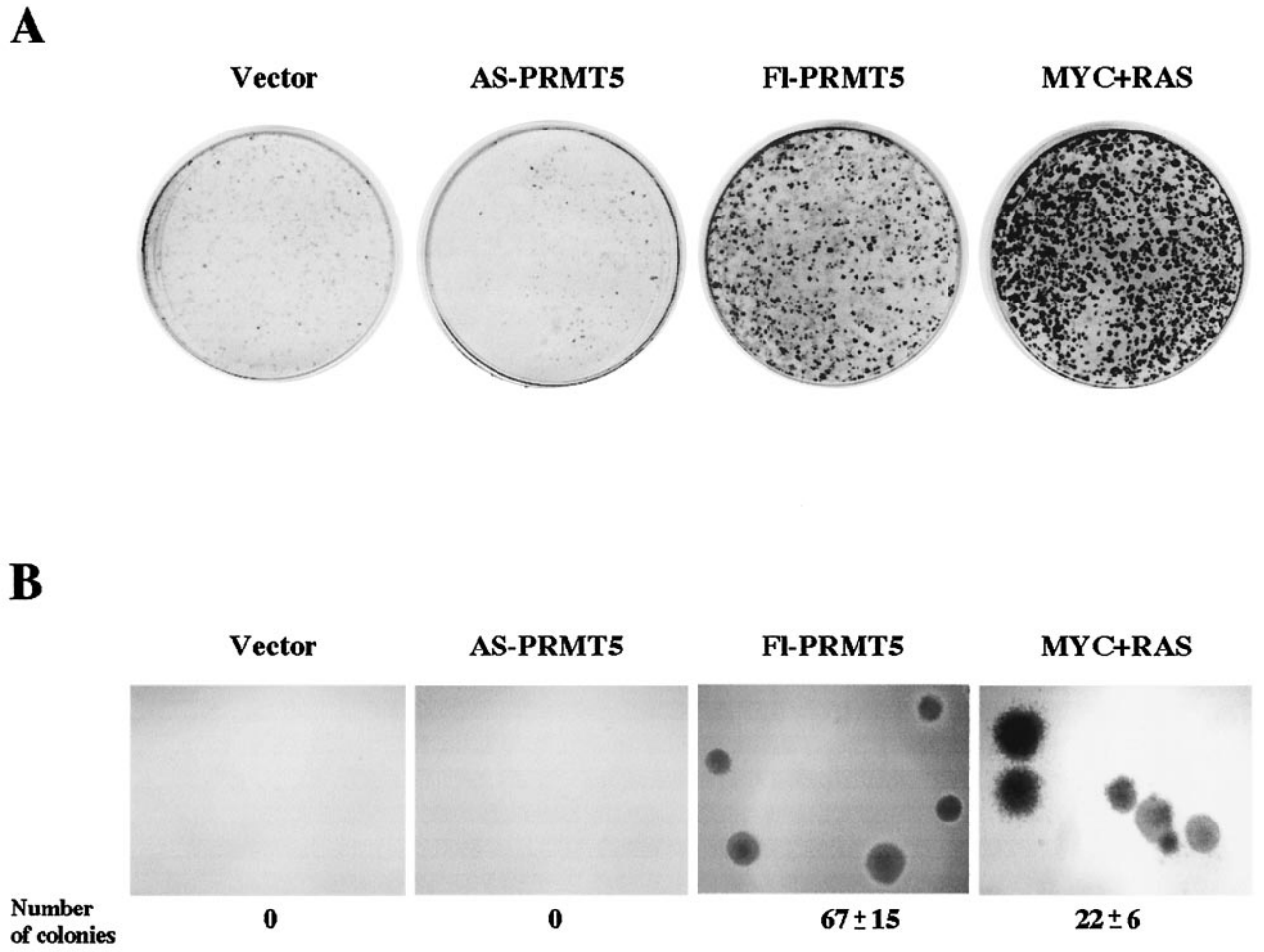

FIG. 6. Overexpression of PRMT5 stimulates anchorage-dependent and -independent growth. (A) Approximately 4×10^3 cells of either puromycin-resistant NIH 3T3, AS-PRMT5, Fl-PRMT5, or hygromycin-resistant MYC/RAS-transformed cell lines were grown in medium containing 10% fetal bovine serum, and after 7 days colonies were stained with crystal violet. (B) Equal numbers (2×10^2) of cells of drug-resistant cell lines containing either vector alone, AS-PRMT5, Fl-PRMT5, or MYC and RAS were grown in soft agar for 10 days. Representative pictures showing the morphology and size of transformed cells are shown at an approximately 35× magnification. Colony formation assays were performed in triplicate and repeated three times. The number shown below each figure represents the average number of colonies from nine plates.

dent manner. Moreover, overexpression of Fl-PRMT5 increased the number of colonies by threefold in comparison to MYC/RAS-transformed NIH 3T3 cells (Fig. 6B). These results show that PRMT5 can stimulate cell growth and proliferation and induce transformation.

PRMT5 directly targets *ST7* and *NM23* tumor suppressor genes. Previous work has shown that recruitment of PRMT5 to the promoter region of target genes correlates with transcriptional repression (7, 20, 32). To gain more insight into the mechanism by which PRMT5 regulates cell proliferation and induces transformation, we analyzed expression of genes identified by microarray analysis in NIH 3T3, AS-PRMT5, and Fl-PRMT5 cell lines (Fig. 7A). We focused on *ST7* and *NM23* because we were able to confirm by RT-PCR that both genes were derepressed in the AS-PRMT5 cell line (Fig. 4C). Moreover, reduced expression of both tumor suppressor genes has been shown to be associated with a wide variety of cancers including breast, prostate, ovarian, colon, head and neck, gastric, pancreatic, and renal cell carcinomas (14, 23, 24, 52, 56). We also examined expression of *myelin transcription factor 1-like* (*MYT1l*), whose expression was deficient in AS-PRMT5 cells. As expected, *ST7* and *NM23* were up-regulated 2.5- and 3.8-fold in the AS-PRMT5 cell line, respectively, while *MYT1l* was down-regulated fivefold (Fig. 7A). When we examined the steady-state level of *ST7*, *NM23*, and *MYT1l* transcripts in cells that overexpress Fl-PRMT5, we found that both *ST7* and *NM23* were repressed, two- and fourfold, respectively. This is consistent with the antisense results and earlier observations, which demonstrated that PRMT5 is involved in transcriptional repression (7, 32). When we examined *MYT1l* expression in the Fl-PRMT5 cell line, we found that its levels increased five- to sixfold, suggesting that PRMT5 is also involved in inducing gene expression.

Not all genes identified may turn out to be direct targets of PRMT5. Some genes may be regulated by indirect mechanisms. Using ChIP assays, we analyzed whether PRMT5 was directly involved in transcriptional regulation of *ST7*, *NM23*, and *MYT1l* (Fig. 7B). Endogenous PRMT5 was associated with the promoter regions of *ST7* and *NM23*, which were up-regulated when PRMT5 levels were reduced. When we evaluated

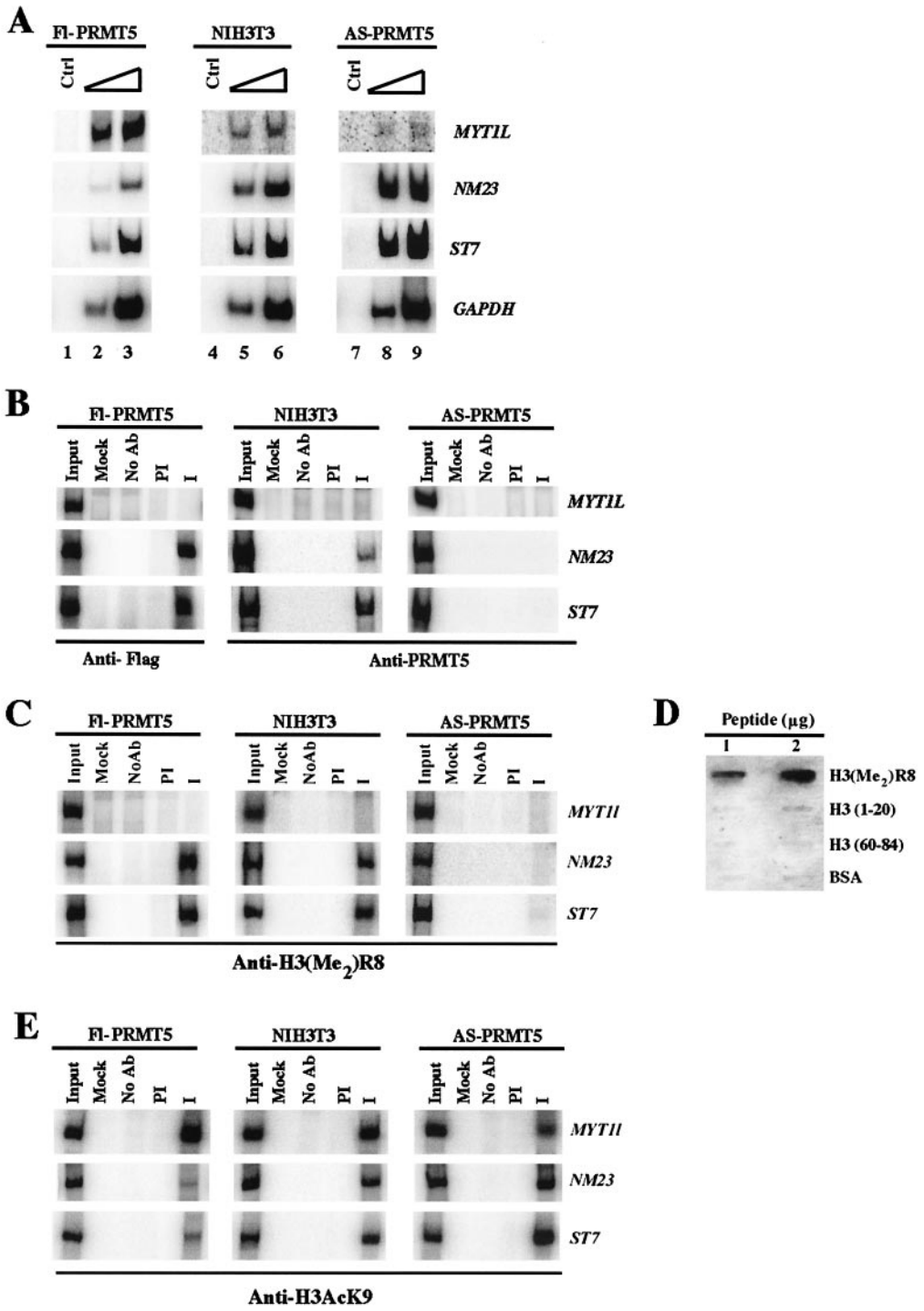

FIG. 7. BRG1- and hBRM-associated PRMT5 is directly involved in transcriptional repression of *ST7* and *NM23*. (A) RT-PCR was performed on 10 μg of total RNA from either Fl-PRMT5, NIH 3T3, or AS-PRMT5 cell lines with primers specific for *MYT1l*, *NM23*, *ST7*, and *GAPDH*. PCR for each gene was carried out using either 2 μl (lanes 1, 3, 4, 6, 7, and 9) or 0.2 μl (lanes 2, 5, and 8) of the RT reaction mixture. Ctrl represents PCRs without 5′ primer (lanes 1, 4, and 7). (B, C, and E) ChIP assays were conducted using cross-linked chromatin from either Fl-PRMT5, NIH 3T3, or AS-PRMT5 cells as described in Materials and Methods with either preimmune (PI) or immune (I) anti-PRMT5 or anti-flag antibodies (B), anti-H3(Me_2)R8 antibodies (C), or anti-H3AcK9 antibodies (E). As controls, mock (reaction mixture without chromatin) and no-antibody (Ab) (reaction mixture with chromatin but without antibody) reactions are shown. For mock, no-Ab, PI, and I reactions, 10 μl of eluted DNA was amplified and 15 μl of each PCR mixture was analyzed. For the input lane, 0.6 μl of eluted DNA was PCR amplified and 10 μl was loaded on the gel. Specific primer pairs were used to amplify *MYT1l* (−258 to +214), *NM23* (−211 to +254), and *ST7* (−228 to +209) sequences. (D) Specificity of anti-H3(Me_2)R8 was determined by Western blot analysis with 1 and 2 μg of symmetrically methylated H3R8 peptide, unmethylated N-terminal and internal H3 peptides, or BSA.

association of PRMT5 with the *ST7* and *NM23* promoters in the antisense cell line, there was a lack of PRMT5 recruitment. In marked contrast, in cells that overexpress Fl-PRMT5 there was recruitment of exogenously expressed PRMT5, which was accompanied by increased *ST7* and *NM23* transcriptional repression (compare panels A and B in Fig. 7). ChIP experiments also revealed that, unlike *ST7* and *NM23*, endogenous PRMT5 and Fl-PRMT5 were not associated with the *MYT1l* promoter, indicating that *MYT1l* is not a direct target of PRMT5.

PRMT5 methylates H3R8 at the *ST7* and *NM23* promoter regions and inhibits H3K9 acetylation. Although PRMT5 was localized to the *ST7* and *NM23* promoter regions, it was not clear whether it could methylate histones. Having established that H3R8 was preferentially methylated by PRMT5 in vitro, we examined the methylation status of this residue at the *ST7*, *NM23*, and *MYT1l* promoter regions. ChIP assays were conducted using antibodies that can specifically recognize symmetrically dimethylated H3R8 but not unmethylated H3 peptides (Fig. 7D). When anti-H3(Me_2)R8 antibodies were incubated with cross-linked chromatin from NIH 3T3 cells, both *ST7* and *NM23* were detected but not *MYT1l* (Fig. 7C). Similarly, when chromatin from cells that overexpress Fl-PRMT5 was immunoprecipitated using anti-H3(Me_2)R8, *ST7* and *NM23* promoter sequences were detected, whereas *MYT1l* sequences were not. However, when ChIP assays were conducted using chromatin from AS-PRMT5 cells, anti-H3(Me_2)R8 failed to immunoprecipitate the *ST7* and *NM23* promoter regions. These results along with the microarray and RT-PCR data, which show that *ST7* and *NM23* are derepressed when PRMT5 levels are reduced, suggest that methylation of H3R8 plays an essential role in transcriptional repression of *ST7* and *NM23* tumor suppressor genes.

In vitro histone N-terminal tail methylation assays revealed that H3K9 acetylation inhibits arginine 8 methylation (Fig. 3E). To assess whether acetylation of H3K9 can affect H3R8 methylation and vice versa, we examined the levels of H3K9 acetylation in NIH 3T3 cells, as well as NIH 3T3 cells that express Fl-PRMT5 and AS-PRMT5 (Fig. 7E). In concordance with the in vitro methylation assays, H3K9 acetylation was inhibited in cells that overexpress Fl-PRMT5, while in AS-PRMT5 cells H3K9 acetylation was readily detectable at the *ST7* and *NM23* promoters. Thus, these findings show that there is negative cross talk between H3K9 acetylation and H3R8 methylation.

***ST7* and *NM23* tumor suppressors are direct targets of BRG1- and hBRM-based hSWI/SNF complexes.** We have shown that PRMT5 can be found in association with BRG1 and hBRM-based hSWI/SNF complexes (Fig. 1 and 2) (32). Therefore, we tested whether BRG1 and hBRM are also recruited to the promoter region of PRMT5 target genes (Fig. 8). Using cross-linked chromatin from either Fl-PRMT5, NIH 3T3, or AS-PRMT5 cells, we found that BRG1 was associated with *ST7* and *MYT1l* but not *NM23* (Fig. 8A). Analysis of hBRM recruitment revealed that it is associated with *MYT1l* and *NM23* but not *ST7* (Fig. 8B). Unlike BRG1, whose recruitment to the *ST7* promoter region is independent of PRMT5 levels, interaction of hBRM with the *NM23* promoter appeared to rely on the presence of PRMT5 (compare Fl-PRMT5, NIH 3T3, and AS-PRMT5 panels). Collectively, these results demonstrate that different genes require distinct PRMT5-containing chromatin remodeling complexes for their regulation.

To verify whether BRG1- and hBRM-based hSWI/SNF complexes can affect *ST7*, *NM23*, and *MYT1l* expression, we analyzed the transcript levels of these direct target genes in cells that express either catalytically inactive BRG1 or hBRM (Fig. 8C). Both *ST7* and *MYT1l* were derepressed in the presence of mutant BRG1 two- to three- and threefold, respectively (Fig. 8D). *MYT1l* was also derepressed 2.5-fold in cells that express catalytically inactive hBRM; however, *NM23* was unaffected in mutant hBRM cells. These results suggest that, while certain PRMT5 target genes are directly affected by BRG1 and hBRM chromatin remodelers, others might be regulated by more elaborate mechanisms.

DISCUSSION

We have previously shown using cell lines that express either flag-tagged BRG1 or hBRM that PRMT5 is tightly associated with flag-tagged hSWI/SNF complexes (32). In this study, we have provided more evidence to show that PRMT5 interacts with endogenous BRG1- and hBRM-based hSWI/SNF complexes purified from either HeLa or flag-tagged INI1 cell lines. We have also shown that hSWI/SNF-associated PRMT5, like recombinant PRMT5, can specifically methylate histones H3 and H4. Mutation of either H3R8 or H4R3 to alanine abolished methylation of histone N-terminal tails, demonstrating that both residues are preferred sites of methylation by recombinant and hSWI/SNF-associated PRMT5. We have identified by microarray analysis PRMT5 target genes and shown that PRMT5 controls cell growth and proliferation by modulating expression of both cell cycle inducers and tumor suppressor genes. Using sense and antisense cell lines, we have shown that BRG1- and hBRM-associated PRMT5 is directly involved in transcriptional repression of *ST7* and *NM23* anticancer genes. Our findings suggest that PRMT5 controls cell growth and proliferation by maintaining appropriate levels of tumor suppressor genes.

PRMT5 targets specific arginine residues in the H3 and H4 N-terminal tails. H3 and H4 N-terminal tails contain highly conserved residues, which can be acetylated, methylated, or phosphorylated. Recent work has shown that acetylation and/or methylation of specific lysine and arginine residues plays a critical role in transcriptional regulation (2, 7, 30, 31, 38, 51). In addition, there appears to be a certain level of interplay between modified sites such that the net result is to either enhance or repress transcription (15, 25, 36, 46). Regulation of chromatin accessibility via histone lysine modification has been studied extensively, and it is becoming evident that the same principles that govern histone lysine acetylation and/or methylation might apply to histone arginine methylation.

We have previously shown that hyperacetylated H3 and H4 are not methylated efficiently by recombinant and hSWI/SNF-associated PRMT5, suggesting that lysine acetylation might interfere with arginine methylation (32). Consistent with this notion, we have found using modified N-terminal H3 peptides that acetylation of H3K9 or K14 blocks H3R8 methylation (Fig. 3E). Moreover, we have shown that there is a certain level of cross talk between H3K9 acetylation and H3R8 methylation in vivo (Fig. 7C and E). Although it is not clear how PRMT5

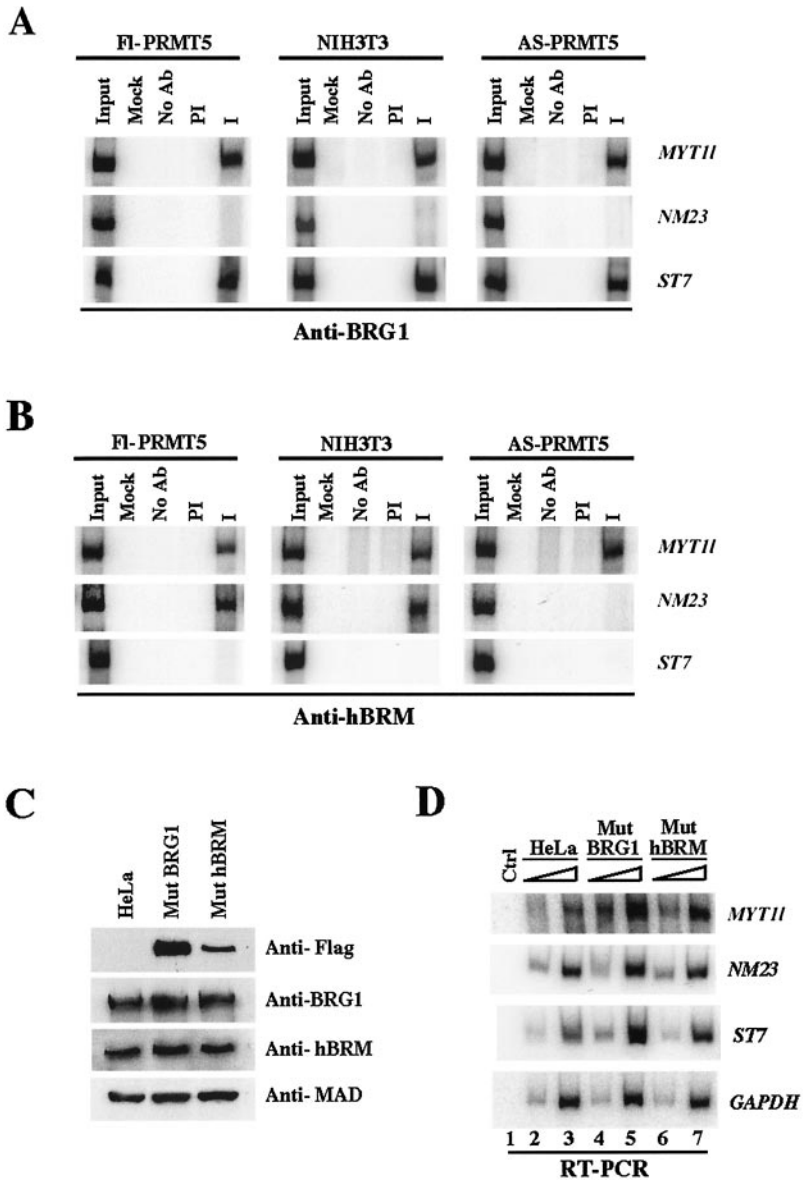

FIG. 8. BRG1 and hBRM are differentially recruited to methylated *ST7* and *NM23* promoters. Cross-linked chromatin was prepared from asynchronous Fl-PRMT5, NIH 3T3, and AS-PRMT5 cell lines, and ChIP assays were conducted as described for Fig. 7 with either preimmune (PI) or immune (I) anti-BRG1 (A) and anti-hBRM (B) antibodies. As controls, mock and no-antibody (Ab) reactions are shown. (C) Levels of catalytically inactive BRG1 and hBRM were measured by Western blotting with 30 μg of nuclear extract from either mutant (Mut) BRG1 or hBRM cell lines. HeLa S3 nuclear extract was used as a control, and proteins were detected using the indicated antibodies. (D) *MYT1l*, *NM23*, *ST7*, and *GAPDH* transcript levels were analyzed by RT-PCR as described for Fig. 7A with RNA from either HeLa cells or HeLa cells that express either mutant BRG1 or hBRM. PCRs were carried out using either 2 μl (lanes 1, 3, 5, and 7) or 0.2 μl (lanes 2, 4, and 6) of the RT reaction mixture. Ctrl represents PCRs without 5′ primer (lane 1).

might repress transcription, it is possible that methylation of H3R8 might sterically hinder accessibility to K9 and limit its accessibility to activating acetyltransferases. This mechanism would provide another way to keep H3K9 hypoacetylated and transcription repressed. It is important to note that PRMT5 also targets H4R3 (GRG), which is known to be methylated by the transcriptional activator PRMT1 (51). In this case, a different mechanism of regulation might be at play. When H4R3 is monomethylated, PRMT5 would catalyze its symmetric dimethylation. Alternatively, if H4R3 is not methylated, PRMT5 would still be able to drive the reaction toward symmetric dimethylation. In either scenario conversion of H4R3 from an unmethylated or monomethylated form to a symmetrically dimethylated form would change its transcriptional activation potential and render it transcriptionally inert.

We have identified the arginine residues targeted by PRMT5 and shown that H3R8 and H4R3 are preferentially methylated by both recombinant and hSWI/SNF-associated PRMT5. Methylation of H3 and H4 N-terminal tails is specific, as both BSA and an internal H3 peptide, which comprises four arginine residues located within the globular domain of H3, failed to show any methylation. We cannot rule out the possibility

that there are other sites methylated by PRMT5, and attempts to identify additional H3 and H4 sites by liquid chromatography-mass spectrometry have failed due to the low recovery of modified peptides after chromatography.

We have shown that H3R8 is methylated at the *ST7* and *NM23* promoter regions in NIH 3T3 and Fl-PRMT5 cells but not in the AS-PRMT5 cell line. We have also used commercially available anti-H4(Me_2)R3 antibodies in ChIP assays, but we were unable to determine whether H4R3 was methylated. We cannot exclude the possibility that H4R3 is methylated at the *ST7* and *NM23* promoters, especially since commercial anti-H4(Me_2)R3 antibodies have not been tested in ChIP assays. Therefore, it is going to be important to determine whether methylation of H3R8 and H4R3 must occur simultaneously in order to repress *ST7* and *NM23* gene expression or whether methylation of either arginine could be sufficient to induce transcriptional repression. More experiments are required to discern between these possibilities, and we are in the process of developing anti-H4(Me_2)R3 antibodies that will allow us to monitor symmetric methylation of this site at the promoter region of PRMT5 direct target genes.

BRG1- and hBRM-associated PRMT5 regulates cell growth and proliferation by modulating expression of *ST7* and *NM23* tumor suppressor genes. To investigate the role of PRMT5 in transcriptional regulation, we have analyzed global gene expression in AS-PRMT5 cells by microarray analysis. We found that more genes were derepressed when PRMT5 levels were reduced by 90%, consistent with its role in transcriptional repression. We verified differential expression of several genes that were either up- or down-regulated (Fig. 4C and D). Based on the microarray results, we expected the AS-PRMT5 cell line to grow faster than control NIH 3T3 cells, because many cell cycle regulators including *CYCLIN E2*, *CYCLIN B2*, and *CDK4*, whose expression has been shown to be enhanced in many types of human tumors, were up-regulated (33, 37, 54). However, the proliferation results indicated that AS-PRMT5 cells grow twofold slower than NIH 3T3 cells, while cells that overexpress PRMT5 behave like *MYC*/*RAS*-transformed NIH 3T3 cells. Since PRMT5 has been linked to transcriptional repression and since several genes involved in inhibiting malignant growth were also found to be up-regulated in the antisense cell line, we reasoned that PRMT5 might be able to promote growth by decreasing expression of tumor suppressor genes. In fact, analysis of the transcript levels of two of these tumor suppressor genes, *ST7* and *NM23*, in cell lines that express either sense or antisense PRMT5 revealed that both genes were derepressed when PRMT5 levels were reduced and repressed when PRMT5 levels were increased (Fig. 7A).

ST7 was identified as one of the tumor suppressor genes on human chromosome 7q31.1, a region frequently associated with loss of heterozygosity in different human cancers (57). Reintroduction of an intact copy of chromosome 7 has been shown to inhibit tumorigenic growth of the highly malignant human prostate adenocarcinoma PC3 cell line, and analysis of revertant clones confirmed that 7q contains the sequences responsible for tumor suppression. Further mapping of 7q31 and reexpression studies showed that *ST7* is a bona fide tumor suppressor that can inhibit tumorigenicity of PC3 cells in nude mice (56). We have also observed that *NM23* transcript levels were decreased in cells that overexpress PRMT5. Highly metastatic cells display low levels of *NM23*, which exhibits nucleoside diphosphate kinase activity (44). Furthermore, reintroduction of *NM23* into K-1735TK melanoma cells, which are highly metastatic, decreased their ability to form colonies in soft agar and reduced the incidence of primary tumor formation in nude mice (23). These studies demonstrate that *ST7* and *NM23* are involved in tumor suppression and confirm our results which show that, when *ST7* and *NM23* levels are reduced in cells that overexpress PRMT5, their ability to hyperproliferate and form colonies in an anchorage-dependent or -independent manner is enhanced. We are aware that there are other genes whose expression is affected when PRMT5 levels are reduced and that they might also be involved in regulating cell growth and proliferation. Therefore, we are in the process of identifying more direct target genes by cloning genomic sequences bound by PRMT5.

We have shown that PRMT5 is directly involved in *ST7* and *NM23* transcriptional repression. We have also determined that, while BRG1 was specifically recruited to the *ST7* promoter, hBRM was targeted to *NM23*. As a control, we have shown that, although *MYT1l* levels fluctuated in the antisense cell line, PRMT5 was not directly involved in its regulation. In addition, we have found that both BRG1 and hBRM were associated with the *MYT1l* promoter. Using cell lines that express catalytically inactive hBRM, we have shown that *MYT1l* was derepressed, while *NM23* was unaffected. It is not clear why *NM23* expression was not altered in the presence of mutant hBRM. One possible scenario is that expression of mutant hBRM might lead to derepression of a negative regulator, which can inhibit *NM23* expression. Alternatively, a second chromatin remodeler might functionally compensate for hBRM, thereby maintaining transcriptional repression of *NM23*. Further experiments aimed at identifying transcriptional regulators involved in modulating *NM23* expression will help elucidate the role played by hBRM-based hSWI/SNF complex in *NM23* transcriptional regulation. When we examined expression of *ST7* and *MYT1l* in cells that express mutant BRG1, we found that both genes were derepressed, confirming the role of BRG1 in transcriptional repression of direct target genes. The fact that BRG1- and hBRM-associated PRMT5 is involved in transcriptional regulation of anticancer genes makes this type II protein arginine methyltransferase an attractive molecule to target in cancer therapy.

ACKNOWLEDGMENTS

We thank G. Leone for MYC and RAS retroviral expression vectors, R. A. Baiocchi and L. Wang for help with FACS and anchorage-dependent growth analyses, other members of the laboratory for technical help, S. Ackerman for critical reading of the manuscript, and S. Waniger and M. Hirschel from the National Cell Culture Center for growing our cell lines.

This work is supported by the Sidney Kimmel Scholar Award SKF-03-022 and National Cancer Institute grant K01 CA89854 to S.S.

REFERENCES

1. **Bannister, A. J., P. Jegerman, J. F. Partridge, E. A. Miska, J. O. Thomas, R. C. Allshire, and T. Kouzarides.** 2001. Selective recognition of methylated lysine 9 on histone H3 by the HP1 chromo domain. Nature **410:**120–124.
2. **Bernstein, B. E., E. L. Humphrey, R. L. Erlich, R. Schneider, P. Bouman, J. S. Liu, T. Kouzarides, and S. L. Schreiber.** 2002. Methylation of histone H3 Lys 4 in coding regions of active genes. Proc. Natl. Acad. Sci. USA **99:**8695–8700.
3. **Branscombe, T. L., A. Frankel, J. H. Lee, J. R. Cook, Z. Yang, S. Pestka, and**

S. Clarke. 2001. PRMT5 (Janus kinase-binding protein 1) catalyzes the formation of symmetric dimethylarginine residues in proteins. J. Biol. Chem. **276:**32971–32976.
4. **Chen, D., M. Ma, H. Hong, S. S. Koh, M. Huang, B. T. Schurter, D. W. Aswad, and M. R. Stallcup.** 1999. Regulation of transcription by a protein methyltransferase. Science **284:**2174–2177.
5. **Cheng, L., and H. W. Wing.** 2001. Model-based analysis of oligonucleotide arrays: model validation, design issues and standard error application. Genome Biol. **2:**Research00321.1–Research0032.11.
6. **de la Serna, I., K. A. Carlson, D. A. Hill. C. J. Guidi, R. O. Stephenson, S. Sif, R. E. Kingston, and A. N. Imbalzano.** 2000. Mammalian SWI-SNF complexes contribute to activation of the *hsp70* gene. Mol. Cell. Biol. **20:** 2839–2851.
7. **Fabbrizio, E., S. El Messaoudi, J. Polanowska, C. Paul, J. R. Cook, J. H. Lee, V. Negre, M. Rousset, S. Pestka, A. Le Cam, and C. Sardet.** 2002. Negative regulation of transcription by the type II arginine methyltransferase PRMT5. EMBO Rep. **3:**641–645.
8. **Frankel, A., N. Yadav, J. Lee, T. L. Branscombe, S. Clarke, and M. T. Bedford.** 2002. The novel human protein arginine N-methyltransferase PRMT6 is a nuclear enzyme displaying unique substrate specificity. J. Biol. Chem. **277:**3537–3543.
9. **Friesen, W. J., S. Paushkin, A. Wyce, S. Massenet, G. S. Pesiridis, G. Van Duyne, J. Rappsilber, M. Mann, and G. Dreyfuss.** 2001. The methylosome, a 20S complex containing JBP1 and pICln, produces dimethylarginine-modified Sm proteins. Mol. Cell. Biol. **21:**8289–8300.
10. **Fry, C. J., and C. L. Peterson.** 2001. Chromatin remodeling enzymes: who's on first? Curr. Biol. **11:**R185–R197.
11. **Gapuzan, M. E., P. V. Yufit, and T. D. Gilmore.** 2002. Immortalized embryonic mouse fibroblasts lacking the RelA subunit of transcription factor NF-κB have a malignantly transformed phenotype. Oncogene **21:**2484–2492.
12. **Gilbreth, M., P. Yang, G. Bartholomeusz, R. A. Pimental, S. Kansra, R. Gadiraju, and S. Marcus.** 1998. Negative regulation of mitosis in fission yeast by the shk1 interacting protein skb1 and its human homolog, Skb1Hs. Proc. Natl. Acad. Sci. USA **95:**14781–14786.
13. **Gilbreth, M., P. Yang, D. Wang, J. Frost, A. Polverino, M. H. Cobb, and S. Marcus.** 1996. The highly conserved skb1 gene encodes a protein that interacts with Shk1, a fission yeast Ste20/PAK homolog. Proc. Natl. Acad. Sci. USA **93:**13802–13807.
14. **Hamby, C. V., C. E. Mendola, L. Potla, G. Stafford, and J. M. Backer.** 1995. Differential expression and mutation of NME genes in autologous cultured human melanoma cells with different metastatic potentials. Biochem. Biophys. Res. Commun. **211:**579–585.
15. **Heard, E., C. Rougeulle, D. Arnaud, P. Avner, C. D. Allis, and D. L. Spector.** 2001. Methylation of histone H3 at Lys-9 is an early mark on the X chromosome during X inactivation. Cell **107:**727–738.
16. **Huang, Y., M. Prasad, W. J. Lemon, H. Hampel, F. A. Wright, K. Kornacker, V. LiVolsi, W. Frankel, R. T. Kloos, C. Eng, N. S. Pellegata, and A. de la Chapelle.** 2001. Gene expression in papillary thyroid carcinoma reveals highly consistent profiles. Proc. Natl. Acad. Sci. USA **98:**15044–15049.
17. **Jenuwein, T., and C. D. Allis.** 2001. Translating the histone code. Science **293:**1074–1080.
18. **Kouzarides., T.** 2002. Histone methylation in transcriptional control. Curr. Opin. Genet. Dev. **12:**198–209.
19. **Kuzmichev, A., Y. Zhang, H. Erdjument-Bromage, P. Tempst, and D. Reinberg.** 2002. Role of the Sin3-histone deacetylase complex in growth regulation by the candidate tumor suppressor $p33^{ING1}$. Mol. Cell. Biol. **22:**835–848.
20. **Kwak, Y. T., J. Guo, S. Prajapati, K. J. Park, R. M. Surabhi, B. Miller, P. Gehrig, and R. B. Gaynor.** 2003. Methylation of SPT5 regulates its interaction with RNA polymerase II and transcriptional elongation properties. Mol. Cell **11:**1055–1066.
21. **Kwon, H., A. N. Imbalzano, P. A. Khavari, R. E. Kingston, and M. R. Green.** 1994. Nucleosome disruption and enhancement of activator binding by a human SW1/SNF complex. Nature **370:**477–481.
22. **Lachner, M., D. O'Carroll, S. Rea, K. Mechtler, and T. Jenuwein.** 2001. Methylation of histone H3 lysine 9 creates a binding site for HP1 proteins. Nature **410:**116–120.
23. **Leone, A., U. Flatow, C. R. King, M. A. Sandeen, I. M. Margulies, L. A. Liotta, and P. S. Steeg.** 1991. Reduced tumor incidence, metastatic potential, and cytokine responsiveness of nm23-transfected melanoma cells. Cell **65:** 25–35.
24. **Leone, A., U. Flatow, K. VanHoutte, and P. S. Steeg.** 1993. Transfection of human nm23-H1 into the human MDA-MB-435 breast carcinoma cell line: effects on tumor metastatic potential, colonization and enzymatic activity. Oncogene **8:**2325–2333.
25. **Lo, W. S., R. C. Trievel, J. R. Rojas, L. Duggan, J. Y. Hsu, C. D. Allis, R. Marmorstein, and S. L. Berger.** 2000. Phosphorylation of serine 10 in histone H3 is functionally linked in vitro and in vivo to Gcn5-mediated acetylation at lysine 14. Mol. Cell **5:**917–926.
26. **Meister, G., C. Eggert, D. Buhler, H. Brahms, C. Kambach, and U. Fischer.** 2001. Methylation of Sm proteins by a complex containing PRMT5 and the putative U snRNP assembly factor pICln. Curr. Biol. **11:**1990–1994.
27. **Nakamura, T., T. Mori, S. Tada, W. Krajewski, T. Rozovskaia, R. Wassell, G. Dubois, A. Mazo, C. M. Croce, and E. Canaani.** 2002. ALL-1 is a histone methyltransferase that assembles a supercomplex of proteins involved in transcriptional regulation. Mol. Cell **10:**1119–1128.
28. **Nakayama, J. I., J. C. Rice, B. D. Strahl, C. D. Allis, and S. I. S. Grewal.** 2001. Role of histone H3 lysine 9 methylation in epigenetic control of heterochromatin assembly. Science **292:**110–113.
29. **Narlikar, G. J., H. Y. Fan, and R. E. Kingston.** 2002. Cooperation between complexes that regulate chromatin and transcription. Cell **108:**475–487.
30. **Nishioka, K., S. Chuikov, K. Sarma, H. Erdjument-Bromage, C. D. Allis, P. Tempst, and D. Reinberg.** 2002. Set9, a novel histone H3 methyltransferase that facilitates transcription by precluding histone tail modifications required for heterochromatin formation. Genes Dev. **16:**479–489.
31. **Noma, K. I., C. D. Allis, and S. I. S. Grewal.** 2001. Transitions in distinct histone H3 methylation patterns at the heterochromatin domain boundaries. Science **293:**1150–1155.
32. **Pal, S., R. Yun, A. Datta, L. Lacomis, H. Erdjument-Bromage, J. Kumar, P. Tempst, and S. Sif.** 2003. mSin3A/histone deacetylase 2- and PRMT5-containing Brg1 complex is involved in transcriptional repression of the Myc target gene *cad*. Mol. Cell. Biol. **23:**7475–7487.
33. **Payton, M., S. Scully, G. Chung, and S. Coats.** 2002. Deregulation of cyclin E2 expression and associated kinase activity in primary breast tumors. Oncogene **21:**8529–8534.
34. **Pollack, B. P., S. V. Kotenko, W. He, L. S. Izotova, B. L. Barnoski, and S. Pestka.** 1999. The human homologue of the yeast proteins Skb1 and Hsl7p interacts with Jak kinases and contains protein methyltransferase activity. J. Biol. Chem. **274:**31531–31542.
35. **Qi, C., J. Chang, Y. Zhu, A. V. Yeldandi, S. M. Rao, and Y. J. Zhu.** 2002. Identification of protein arginine methyltransferase 2 as a coactivator for estrogen receptor alpha. J. Biol. Chem. **277:**28624–28630.
36. **Rea, S., F. Eisenhaber, D. O'Carroll, B. D. Strahl, Z. W. Sun, M. Schmid, S. Opravil, K. Mechtler, C. P. Ponting, C. D. Allis, and T. Jenuwein.** 2000. Regulation of chromatin structure by site-specific histone H3 methyltransferases. Nature **406:**593–599.
37. **Sarafan-Vasseur, N., A. Lamy, J. Bourguignon, F. L. Pessot, P. Hieter, R. Sesboue, C. Bastard, T. Frebourg, and J. M. Flaman.** 2002. Overexpression of B-type cyclins alters chromosomal segregation. Oncogene **21:** 2051–2057.
38. **Schultz, D. C., K. Ayyanathan, D. Negorev, G. G. Maul, and F. J. Rauscher III.** 2002. SETDB1: a novel KAP-1-associated histone H3, lysine 9-specific methyltransferase that contributes to HP1-mediated silencing of euchromatic genes by KRAB zinc-finger proteins. Genes Dev. **16:**919–932.
39. **Schurter, B. T., S. S. C. Koh, D. Chen, G. J. Bunick, J. M. Harp, B. L. Hanson, A. Henschen-Edman, D. R. Mackay, M. R. Stallcup, and D. W. Aswad.** 2001. Methylation of histone H3 by coactivator-associated arginine methyltransferase 1. Biochemistry **40:**5747–5756.
40. **Schwarzler, A., H. J. Kreienkamp, and D. Richter.** 2000. Interaction of the somatostatin receptor subtype 1 with the human homolog of the Shk1 kinase-binding protein from yeast. J. Biol. Chem. **275:**9557–9562.
41. **Sif, S.** 2004. ATP-dependent nucleosome remodeling complexes: enzymes tailored to deal with chromatin. J. Cell. Biochem. **91:**1087–1098.
42. **Sif, S., A. J. Saurin, A. N. Imbalzano, and R. E. Kingston.** 2001. Purification and characterization of mSin3A-containing Brg1 and hBrm chromatin remodeling complexes. Genes Dev. **15:**603–618.
43. **Sif, S., P. T. Stukenberg, M. W. Kirschner, and R. E. Kingston.** 1998. Mitotic inactivation of a human SWI/SNF chromatin remodeling complex. Genes Dev. **12:**2842–2851.
44. **Steeg, P. S., G. Bevilacqua, L. Kopper, U. P. Thorgeirsson, J. E. Talmadge, L. A. Liotta, and M. E. Sobel.** 1988. Evidence for a novel gene associated with low tumor metastatic potential. J. Natl. Cancer Inst. **80:**200–204.
45. **Strahl, B. D., and C. D. Allis.** 2000. The language of covalent histone modifications. Nature **403:**41–45.
46. **Sun, Z. W., and C. D. Allis.** 2002. Ubiquitination of histone H2B regulates H3 methylation and gene silencing in yeast. Nature **418:**104–108.
47. **Tang, J., J. D. Gary, S. Clarke, and H. R. Herschman.** 1998. PRMT 3, a type I protein arginine N-methyltransferase that differs from PRMT1 in its oligomerization, subcellular localization, substrate specificity, and regulation. J. Biol. Chem. **273:**16935–16945.
48. **Tong, J. K., C. A. Hassig, G. R. Schnitzler, R. E. Kingston, and S. L. Schreiber.** 1998. Chromatin deacetylation by an ATP-dependent nucleosome remodelling complex. Nature **395:**917–921.
49. **Wade, P. A., P. A. Jones, D. Vermaak, and A. P. Wolffe.** 1998. A multiple subunit Mi-2 histone deacetylase complex from *Xenopus laevis* cofractionates with an associated Snf2 superfamily ATPase. Curr. Biol. **8:**843–846.
50. **Wang, H., R. Cao, L. Xia, H. Erdjument-Bromage, C. Borchers, P. Tempst, and Y. Zhang.** 2001. Purification and functional characterization of a histone H3-lysine 4-specific methyltransferase. Mol. Cell **8:**1207–1217.
51. **Wang, H., Z. Q. Huang, L. Xia, Q. Feng, H. Erdjument-Bromage, B. D. Strahl, S. D. Briggs, C. D. Allis, J. Wong, P. Tempst, and Y. Zhang.** 2001. Methylation of histone H4 at arginine 3 facilitating transcriptional activation by nuclear hormone receptor. Science **293:**853–857.
52. **Wang, S., Y. Mori, F. Sato, J. Yin, Y. Xu, T. T. Zou, A. Olaru, M. C. Kimos, K. Perry, F. M. Selaru, E. Deacu, M. Sun, Y. C. Shi, D. Shibata, J. M.**

Abraham, B. D. Greenwald, and S. J. Meltzer. 2003. An LOH and mutational investigation of the ST7 gene locus in human esophageal carcinoma. Oncogene **22:**467–470.

53. **Wiley, D. J., S. Marcus, G. D'Urso, and F. Verde.** 2003. Control of cell polarity in fission yeast by association of Orb6p kinase with the highly conserved protein methyltransferase Skb1p. J. Biol. Chem. **278:**25256–25263.
54. **Wolfel, T., M. Hauer, J. Schneider, M. Serrano, C. Wolfel, E. Klehmann-Hieb, E. De Plaen, T. Hankeln, K. H. Meyer zum Buschenfelde, and D. Beach.** 1995. A p16INK4a-insensitive CDK4 mutant targeted by cytolytic T lymphocytes in a human melanoma. Science **269:**1281–1284.
55. **Xue, Y., J. Wong, G. T. Moreno, M. K. Young, J. Cote, and W. Wang.** 1998. NURD, a novel complex with both ATP-dependent chromatin-remodeling and histone deacetylase activities. Mol. Cell **2:**851–861.
56. **Zenklusen, J. C., C. J. Conti, and E. D. Green.** 2001. Mutational and functional analyses reveal that ST7 is a highly conserved tumor-suppressor gene on human chromosome 7q31. Nat. Genet. **27:**392–398.
57. **Zenklusen, J. C., L. C. Hodges, M. LaCava, E. D. Green, and C. J. Conti.** 2000. Definitive functional evidence for a tumor suppressor gene on human chromosome 7q31.1 neighboring the Fra7G site. Oncogene **19:**1729–1733.
58. **Zhang, Y., and D. Reinberg.** 2002. Transcription regulation by histone methylation: interplay between different covalent modifications of the core histone tails. Genes Dev. **15:**2343–2360.
59. **Zhang, Y., G. LeRoy, H. P. Seelig, W. S. Lane, and D. Reinberg.** 1998. The dermatomyositis-specific autoantigen Mi2 is a component of a complex containing histone deacetylase and nucleosome remodeling activities. Cell **95:** 279–289.